EXPERIMENTAL BEHAVIOR OF HIGH STRENGTH CONCRETE SLABS SUBJECTED TO SHOCK LOADING

A THESIS IN

Civil Engineering

Presented to the Faculty of the University of
Missouri at Kansas City in partial fulfillment of
the requirements of the degree

MASTER OF SCIENCE

by

KRISTEN ASHLEY REYNOLDS

B.S. University of Missouri – Columbia, 2013

Kansas City, Missouri

2015

EXPERIMENTAL BEHAVIOR OF HIGH STRENGTH CONCRETE SLABS SUBJECTED TO SHOCK LOADING

Kristen Ashley Reynolds, Candidate for the Master of Science Degree
University of Missouri at Kansas City, 2015

ABSTRACT

The design to resist blast loading is required in many private and governmental buildings. The research presented in this thesis characterizes the response of high strength concrete panels, reinforced with high strength vanadium steel, subjected to blast loading under controlled conditions. This work is intended to provide valuable data to study numerical models such as the commonly used single-degree-of-freedom (SDOF) models. The experimental procedure used and data collected from high-strength reinforced concrete (RC) slabs, having two different high-strength reinforcement ratios subjected to shockwave loadings using a blast load simulator are presented in this thesis. The pressure, impulse, and deflection time histories generated from the experiments along with the predicted panel deflection and damage responses are presented. The pressure impulse (PI) curves developed using a SDOF model are compared with the experimental data. Damage assessment generated from the blast load simulator experiments and a comparison of experimental behavior of high strength RC slabs with regular strength RC slabs, having two different Grade 60 regular-strength reinforcement ratios, are also presented. These results showed that while the regular strength slabs with regular strength reinforcing steel experienced slightly higher experimental deflections that the high strength slabs with high strength reinforcing

steel, the reinforcement spacing or reinforcement ratio, played a more significant role in both experimental and numerical maximum peak deflections for both the regular strength concrete slabs reinforced with regular strength steel and the high strength concrete slabs reinforced with high strength steel. Experimental quantification of the dynamic resistance curves showed that the slabs with smaller longitudinal reinforcement spacing had greater ductility and post-yield behavior. Furthermore, a parametric study was performed, using the same SDOF model, comparing various high-strength concrete slab thicknesses with varying high-strength reinforcement ratios for maximum numerical deflection. The results from this study showed that the thicker slabs with larger reinforcement ratios yielded smaller maximum numerical deflections than those of the thinner slabs with smaller reinforcement ratios. Finally, the concrete damage patterns of the panels are shown and described.

APPROVAL PAGE

The faculty listed below, appointed by the Dean of the School of Computing and Engineering have examined a thesis titled “Experimental Behavior of High Strength Concrete Slabs Subjected to Shock Loading” presented by Kristen Ashley Reynolds, candidate for the Master of Science degree, and certify that in their opinion it is worthy of acceptance.

Supervisory Committee

Ganesh Thiagarajan, Ph.D., P.E., Committee Chair
Department of Civil and Mechanical Engineering

Ceki Halmen, Ph.D.
Department of Civil and Mechanical Engineering

ZhiQiang Chen, Ph.D.
Department of Civil and Mechanical Engineering

TABLE OF CONTENTS

LIST OF TABLES

LIST OF ILLUSTRATIONS

ACKNOWLEDGEMENTS

Throughout the duration of my graduate education at the University of Missouri – Kansas City, I have been fortunate to receive guidance and support from numerous persons with a vested interest in my educational and personal aspirations. I must first acknowledge my advisor and Major Professor, Dr. Ganesh Thiagarajan. Thank you, Dr. Ganesh, for consistently challenging me while always being such a positive and supportive influence in my life. Also, thank you for the extensive time and dedication you put into advising my research and assisting me in my career endeavors. Being mentored by you throughout my graduate experience has been such a privilege and I cannot thank you enough.

My sincere thanks also goes to the rest of my thesis committee: Dr. Chen and Dr. Halmen, not only for their insightful comments and encouragement, but also for always challenging me throughout my graduate education.

Additionally, I want to thank my family for their love and support. My parents raised me to believe that I could achieve anything I set my mind to. My mother, especially, has been there for me throughout this journey. Without her, I would not be where I am today. To my grandparents, Gammy and Paca, I want to thank you for always being there for me through every crisis, and for your endless source of great joy and love. To my future family-in-law, the Stehls, thank you for not letting me forget to have fun, even in tough times, and for reminding me what unconditional love and family is all about. And, finally, to my fiancé and best friend, Austin Stehl. You are my rock and my everything. Without you, I would not have been able to do any of this. I love you so very much.

CHAPTER 1

INTRODUCTION

World events in the past few years have highlighted the need to ensure our civilian and military buildings and their components are designed to withstand the rigors of extreme loadings. Reinforced concrete (RC), as a structural material, is effective in withstanding the effects of shock loading due to blast waves and penetration effects due to impact loading.

The response of concrete structures to blast loading depends on the nature of the blast, geometric and dynamic structural characteristics, and material dynamic response characteristics. The loading regime is characterized by using the scaled distance Z, defined as the ratio of the standoff distance to the cube root of the charge weight, and is classified as close-in, near field, or far field (1) depending on the value of Z. Based on the scaled distance of the explosion, the pressure histories on different parts of the structure can be computed using principles of shock physics (2). For design purposes, the characteristics of loading include the peak reflected and side on pressure and the duration of loading or the impulse imparted to the structure (3). The structural response to the explosion depends on the natural time period of the structure, the boundary conditions, and the ratio of the load duration to the natural period of the structure. The response can be characterized as impulsive, dynamic, or quasi-static (1). The material dynamic response often displays an increased enhanced strength due to strain rate effects (4), which is characterized by dynamic increase factors applied to the strength of concrete and steel yield stresses (5). The research presented in this thesis provides experimental data related to the structural response of high strength concrete (15 ksi) slabs reinforced with

Vanadium steel (83 ksi) subjected to shock loading and studies their benefits in comparison to normal strength RC slabs.

CHAPTER 2

LITERATURE REVIEW

Previous blast reinforced concrete slab studies (6-8) demonstrate the pressing need to validate and characterize data from the experimental response of reinforced high-strength concrete slabs when subjected to blast loading. Wu et al. (9) studied the behavior of FRP retrofitted slabs and ultra-high performance concrete slabs subjected to blast loading and found that the ultra-high performance concrete slabs, without reinforcement, suffered less damage compared to normal RC slabs, suggesting that ultra-high performance concrete is a more suitable material for blast design. Kim et al. (7) performed blast tests to investigate the behavior of Ultra High Strength Concrete (UHSC) and Reactive Powder Concrete (RPC) slabs when subjected to blast loading and showed that both UHSC and RPC effectively resist blast explosions compared to normal concrete. Yun and Park (8) numerically investigated the blast damage behavior of reinforcing bars embedded in a High Strength Concrete (HSC) slab subjected to blast loading. Equation of state, strength, and failure models of materials were implemented in their analysis to enhance the accuracy of the simulation results and, when compared to reported experimental results, were found to be in good agreement. Hao and Zhongxian (10) numerically studied the dynamic behavior of reinforced concrete (RC) slabs under blast loading and its influencing factors taking into account strain rate effects and damage accumulation to investigate the effects that thickness and reinforcement ratio had on the behavior of the slab under blast loading. They found that increasing the slab thickness may

improve the RC slab's blast load carrying capacity and that a higher reinforcement ratio had an unobvious effect on blast-resistant capacity.

A range of techniques, such as single and multi-degree-of-freedom models along with advanced finite element material models, are used to analyze the dynamic response of structures under extreme loading. One of these techniques is applicable for the research presented in this paper; namely the single degree of freedom (SDOF) models.

In SDOF models, the equivalent mass and stiffness of the structure are calculated, which are then used to model the structure as a mass and a spring system having one degree of freedom. Li and Meng (5, 11) have analytically studied the influence of loading shape on the dynamic structural response of SDOF systems. Krauthammer et al. (12, 13) have used advanced SDOF approaches using analytical and numerical methods to study the effects of loading and material behavior on concrete structures. Several well developed programs exist to perform SDOF analysis for structural systems such as the SDOF Blast Effects Design Spreadsheet (SBEDS), which was developed for the Protective Design Center of the United States Army Corps of Engineers (14). Peak pressure and impulse or pressure-time histories due to the applied loading are two important loading characteristics needed for SDOF analysis.

This study is a continuation of the previous work done by Thiagarajan and Johnson (15) examining the structural response of reinforced normal strength concrete slabs subjected to shock loading. Thiagarajan and Johnson (15) performed shockwave-loading tests on normal strength RC slabs that had two different reinforcement ratios, using a blast load simulator, and reported on the experimental procedure used and the data collected. Single degree of freedom (SDOF) numerical models were considered and were validated by using pressure, impulse, and deflection times histories generated from these experiments. SDOF designs proved to be

conservative upon observation of the pressure/impulse (PI) curves developed compared to experimental data. Strains and strain rates experienced by the panels used in the experiments showed a structural dynamic increase factor that ranged from 5 to 10 for tensile strains. Dynamic resistance curves were experimentally quantified showing that slabs with lesser longitudinal reinforcement spacing had greater ductility and post-yield behavior. The results of these experiments compared to the data results presented in this paper.

From the literature survey it can be seen that there is a strong need to characterize the experimental response of reinforced concrete slabs subjected to blast loading and to provide general data for validation of numerical models. Experimental data that would validate the SDOF models commonly used by designers are also needed in order to assess their conservativeness. The experimental and corresponding numerical analysis research data presented in this paper is an attempt to addresses several of these needs.

CHAPTER 3

RESEARCH SIGNIFICANCE

A number of designers use SDOF's that are available for the design of structures subjected to blast loading. However, the challenge lies in using them with a degree of confidence. The significance of the research presented in this paper is the attempt to provide data, from controlled tests for validation of numerical models, which are sparingly available in literature, especially pertaining to pressure, strain, and deflection histories. To address this area of need, four specific aims are addressed in this paper. The first specific aim is to describe experiments conducted on high strength concrete panels, having two different cross sectional areas of vanadium steel reinforcement, using shock tube loadings capable of generating reflective pressures associated with blast events. The second specific aim of this research is to measure strain rates experienced by concrete under blast loading. While it has been reported that concrete structures under blast loading can experience strain rates of the order of 10^3/s or higher (5) few experimental data reporting strain rates during structural response exist. The third specific aim is to measure the damage due to experimentally applied pressure and impulse on the panels and compare them with analytically developed SDOF model-based PI curves to assess the efficacy of the practical methods currently in use. Finally, the fourth specific aim is to compare the results of the experiments for the high strength RC panels, reinforced with two different areas of vanadium steel to the results of the previous and similar experiments for the normal strength RC panels, reinforced with two different areas of regular reinforcing steel.

CHAPTER 4

EXPERIMENTAL INVESTIGATION

Experimental Setup

Dynamic tests were performed on six one-third scale RC panels using the compressed gas-driven blast load simulator (BLS) at the Engineer Research and Development Center (ERDC) located in Vicksburg, MS. This BLS device was also used in experiments done by Thiagarajan and Johnson (15) and consists of a driver or pressure vessel, a vented cone, transition components, and a target vessel. A schematic showing this description of the BLS can be seen in Figure 1. A photograph of the BLS device used in these experiments can also been seen in Figure 1.

Figure 1- Blast Load Simulator (Top) Schematic (Bottom) Photograph

The BLS used in these experiments can simulate an air-blast environment for explosive yields of up to 20,000 lbs. of TNT and generate the positive and negative phase required for blast wave phenomenon. The wave form was created by confining compressed gases (air/helium) in the driver which upon release created a blast wave that propagated downstream through the vented cone to the transition components which then impacted the slabs housed in the target vessel. High-speed cameras and a fully instrumented target vessel were immediately available following the experiments to review the data collected.

The RC panels consisting of a single mat of high-strength, 83 ksi (572.3 MPa), Vanadium reinforcing bars embedded in 15 ksi (103.4 MPa) concrete were pinned within a steel frame that was bolted into the target vessel. These high strength concrete slabs reinforced with vanadium steel are referred to as HSCV slabs. The slabs were set on a cardboard foam-like material that had a compressible honeycomb structure in the blast load simulator. Hollow structural steel (HSS) tubes were placed at the top and the bottom of the slabs on the longitudinal (long) ends of the blast face and were taken as simple supports to prevent the slabs from falling during a possible rebound phase. The slabs were unsupported on the lateral (short) ends since gaps were left between the sides of the slabs and the loading frame. The experimental boundary conditions permitted the classification of slab response as one-way action. Figure 2 demonstrates how the slabs were placed in the blast load simulator for loading.

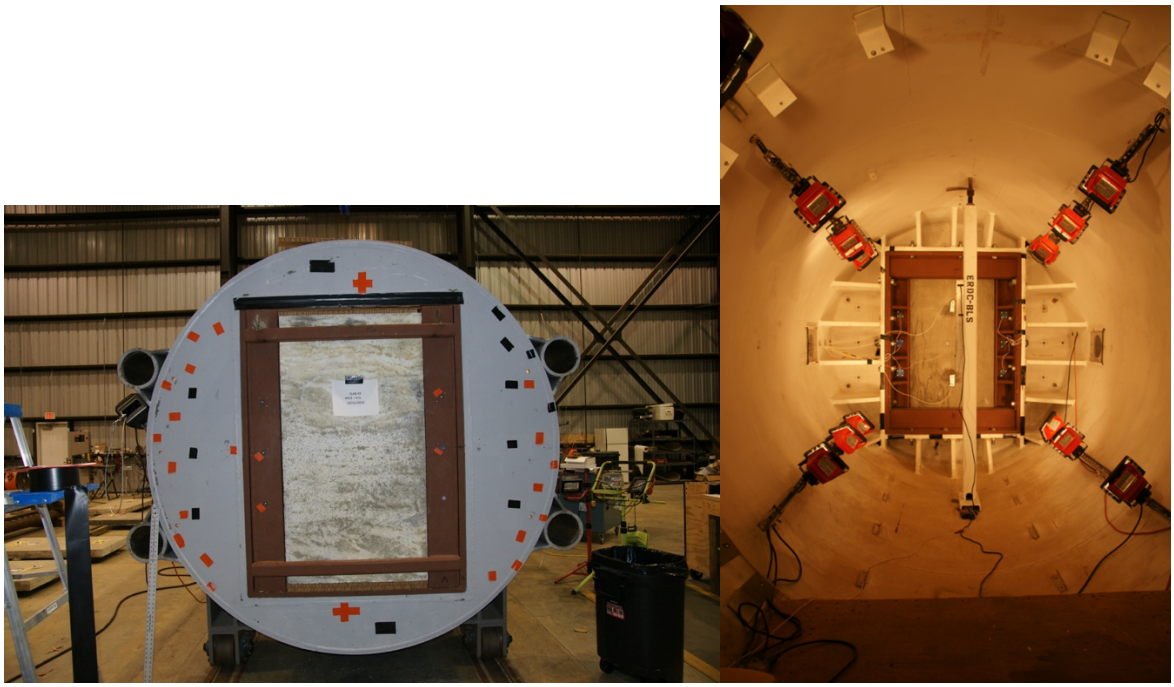

Figure 2- Slab Placement in the Blast Load Simulator (a) Viewed from the Blast Side, (b) Viewed from the Face Opposite the Blast Side

Blast Test Matrix and Specimen Details

Six RC panel specimens each having dimensions of 64 x 36 x 4 in. (1625 x 915 x 101.6 mm) were cast with one layer of vanadium reinforcing steel (1/2 in. [12.7 mm] of clear cover, typical) on the tensile face of the slab. The tensile face is the face opposite the blast face of the slab. The high-strength concrete (HSC) specimen had a compressive strength of 15 ksi (105 MPa). Three panels, termed HSCV1, HSCV2, and HSCV3 were reinforced on the tensile side with No. 3 bars at 4 in. center-to-center (9.5 mm at 101.6 mm); and three panels, termed HSCV4, HSCV5 and HSCV6, had No. 3 bars at 8 in. center-to-center (9.5 mm at 203.2 mm). The 4 in. reinforcement layout is shown in Figure 3 and the 8 in. reinforcement layout is shown in Figure 4. These two panel sets correspond to reinforcement ratios of 0.69% and 0.35%, respectively.

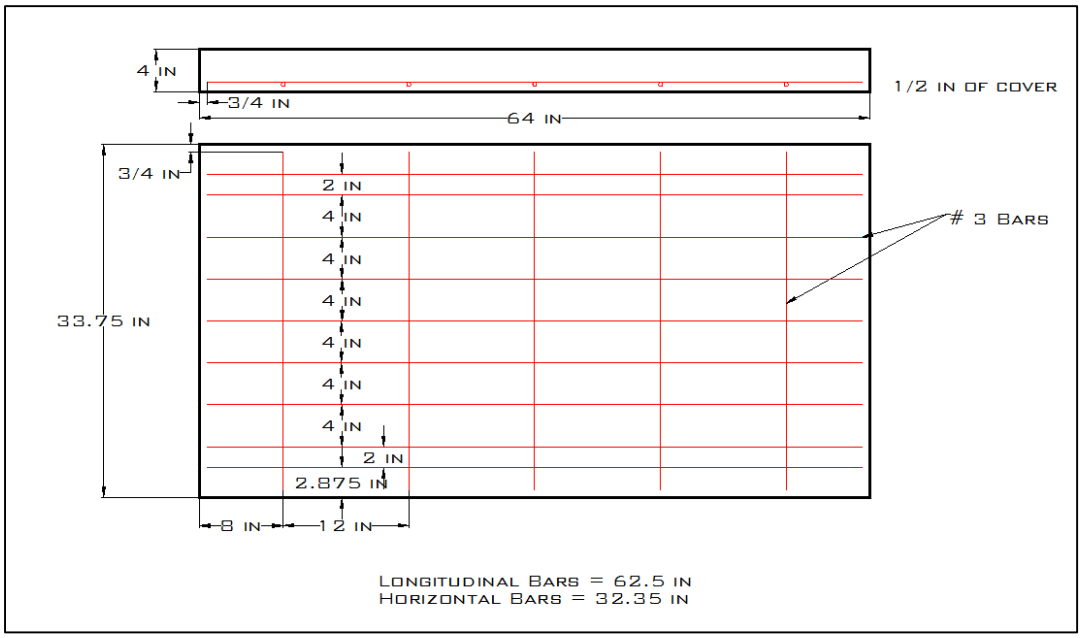

Figure 3- 4 in. Slab Reinforcement Layout

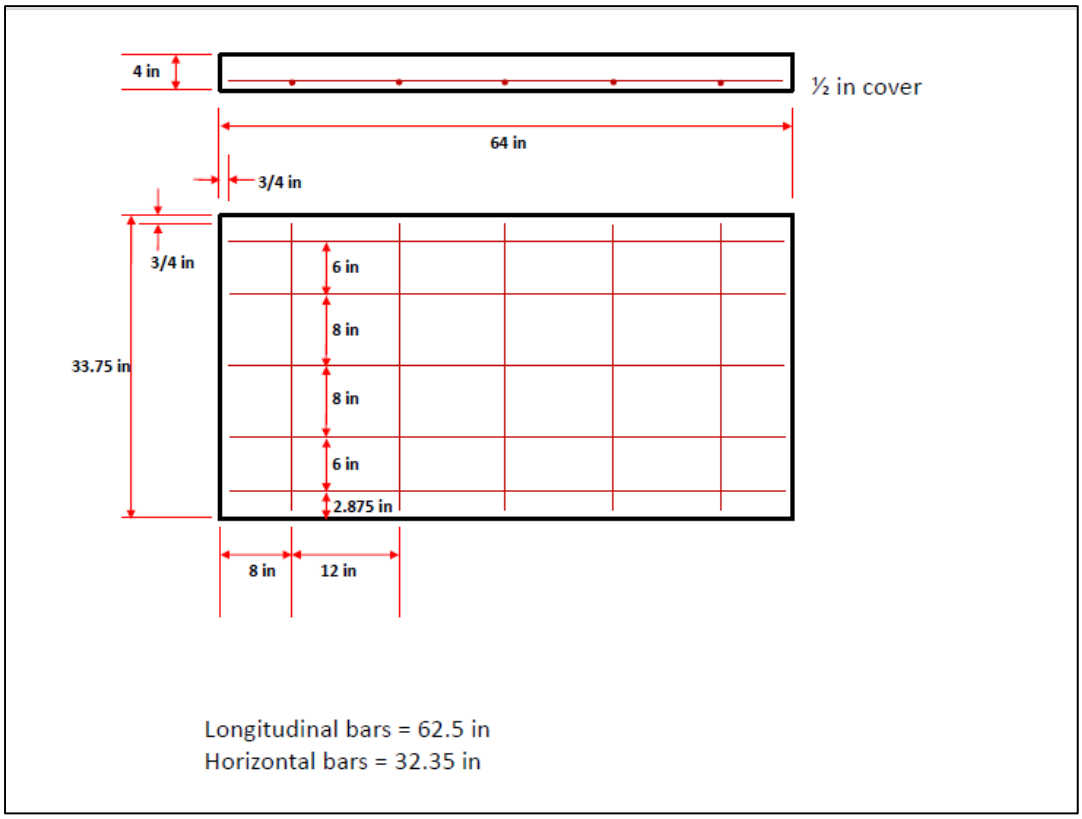

Figure 4- 8 in. Slab Reinforcement Layout

Data Acquisition and Imaging

Displacement data was recorded using a centrally located piezoresistive accelerometer at a sampling rate of 1000 kHz and a laser displacement sensor recording at a 1000 kHz sampling rate pointing at the center of the slab. Reflected pressure data was recorded at six different locations using pressure sensors recording at a 1000 kHz sampling rate embedded in the outer frame of the experimental setup. Figures 5 and 6 show the slab instrumentation plan on the blast face and the side opposite the blast face (the tensile side), respectively. Deformation/damage data were recorded using four high speed digital cameras. Two cameras were placed to view the back of the specimen and two cameras were placed to record the deformation on two sides. The cameras had a rate of 1000 frames per second and were capable of recording up to 8.9 seconds of video depending on the camera resolution. Two Vishay Model N2A-06-20CBW-350/E strain gauges recording at a 1000 kHz sample rate were placed on the tension side of the slab at quarter heights to record strains. The strain gauges were mounted on the concrete surface and were placed at quarter heights to avoid damaging the gauges during the experiment. A photograph of the placement of the pressure sensors and strain gauges on the RC slabs is shown in Figure 7.

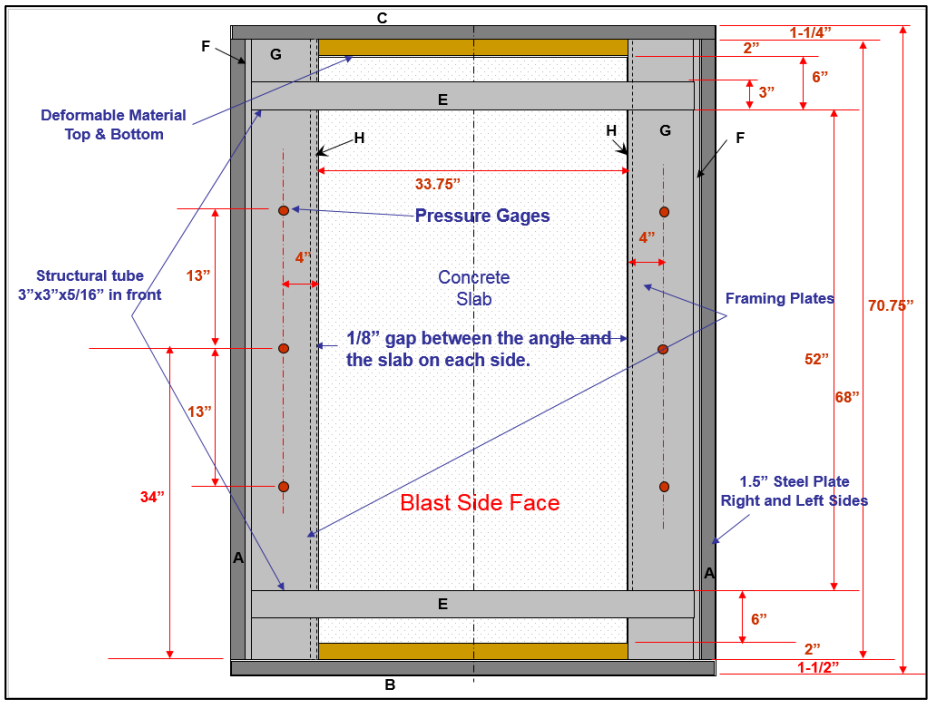

Figure 5- Pressure Sensor Instrumentation Plan on Blast Side Face of the Slab

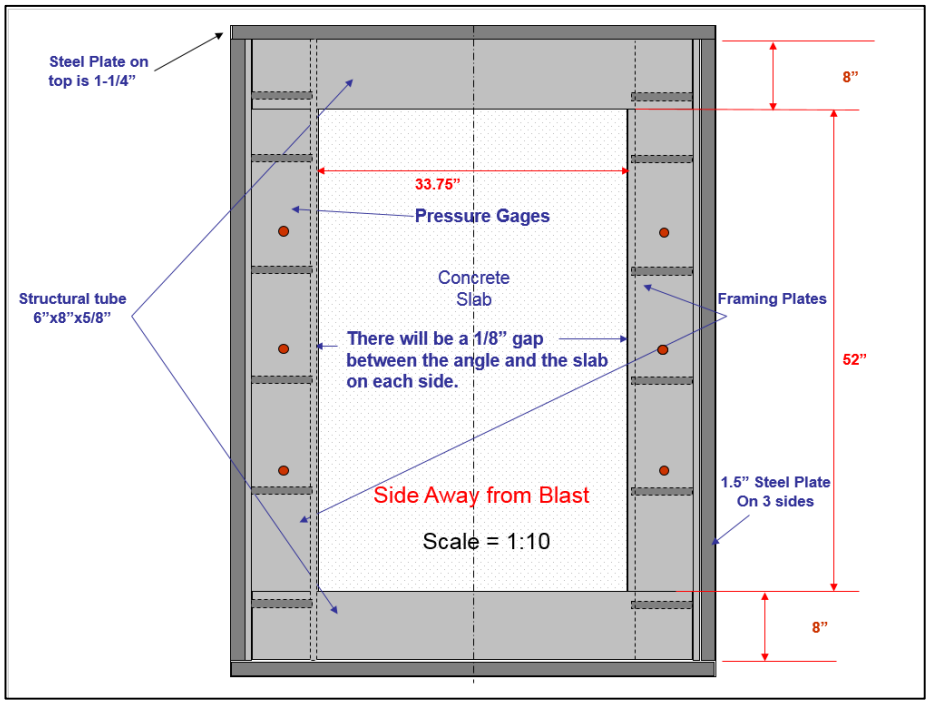

Figure 6- Pressure Sensor Instrumentation Plan on the Side Away from the Blast Face of the Slab

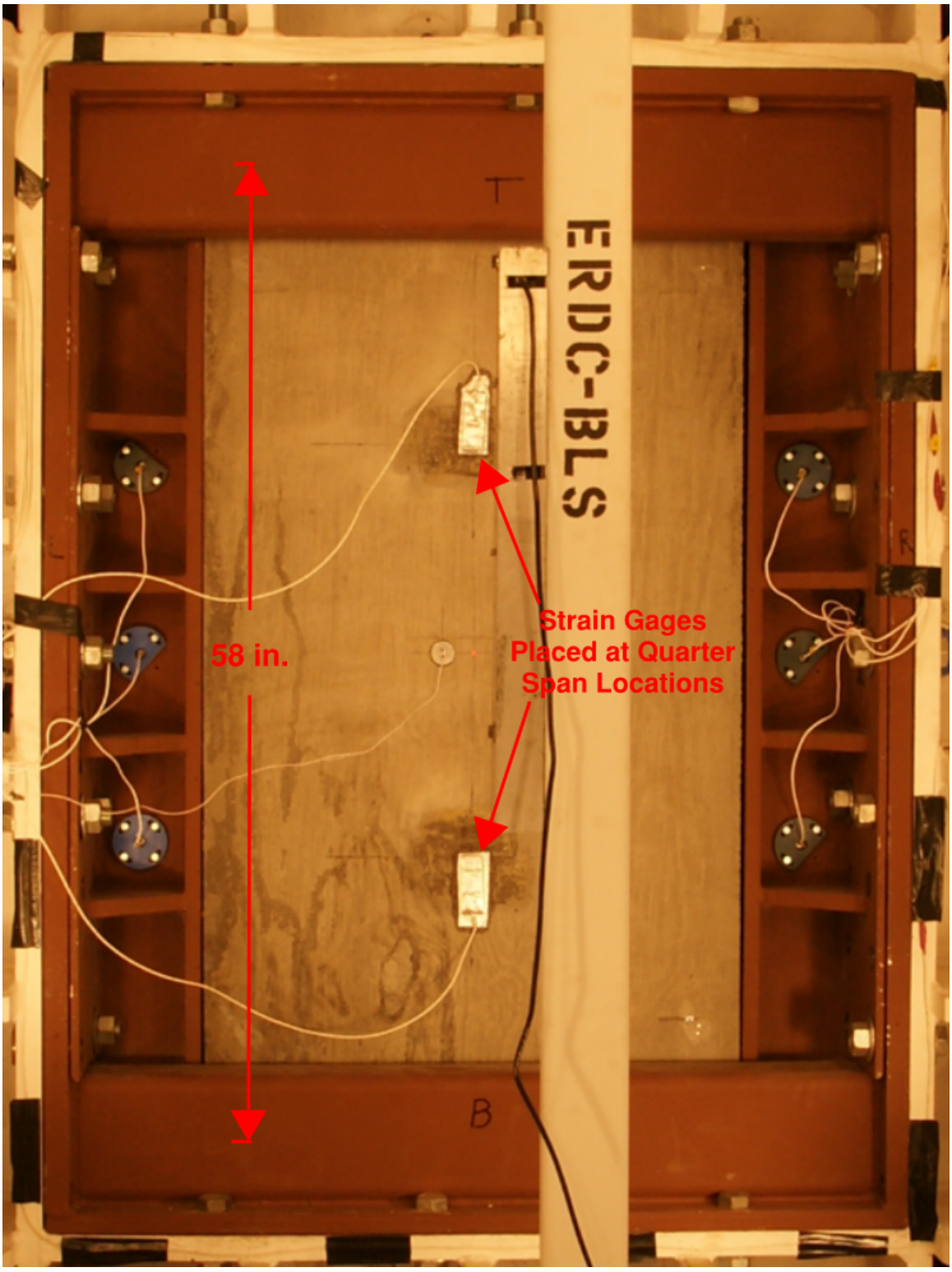

Figure 7- Pressure Sensor and Strain Gauge Placement on Tensile Side of RC Slab in BLS

CHAPTER 5

DATA AND RESULTS

Material Test Properties

A high strength concrete mix with a 15 ksi (103.4 MPa) compressive design strength was used for the HSCV slabs. The fresh properties of the concrete included a slump of 9 in. (228.6 mm), a weight of 156.4 pcf (2,505.3 kg/m^3), an air content of 2.5%, and a temperature of 81°F (27.22 °C). Nine high strength concrete test cylinders were poured. The first 3 cylinders were tested at an age of 14 days, the next 3 cylinders were tested at an age of 28 days, and the final 3 cylinders were tested at an age of 56 days. The cylinders tested at 14 days had an average unconfined compressive strength and an average density of 10,676.67 psi (73.6 MPa) and 152.0 pcf (2,434.8 kg/m^3), respectively. The cylinders tested at 28 days had an average unconfined compressive strength and an average density of 13,473.33 psi (92.9 MPa) and 151.9 pcf (2,433.2 kg/m^3), respectively. The cylinders tested at 56 days had an average unconfined compressive strength and an average density of 15,756.67 psi (108.6 MPa) and 153.2 pcf (2,454 kg/m^3), respectively. The HSCV slabs were reinforced with high-strength Vanadium steel which produced a yield strength of 83 ksi (572.3 MPa) after tensile testing.

The regular strength concrete slabs reinforced with regular strength (Grade 60) steel, studied for this thesis, are referred to as RSCR slabs. A regular strength concrete mix with a 5 ksi (34.5 MPa) compressive design strength was used for the RSCR slabs. The fresh properties of the concrete included a slump of 6.25 in. (158.8 mm), a weight of 149.0 pcf (2,386.8 kg/m^3), an air content of 4.4%, and a temperature of 80°F (26.67 °C). Nine regular strength concrete

test cylinders were poured. The first 3 cylinders were tested at an age of 7 days, the next 3 cylinders were tested at an age of 14 days, and the final 3 cylinders were tested at an age of 28 days. The cylinders tested at 7 days had an average unconfined compressive strength and an average density of 5,040 psi (34.7 MPa) and 148.7 pcf (2,381.9 kg/m^3), respectively. The cylinders tested at 14 days had an average unconfined compressive strength and an average density of 5,380 psi (37.1 MPa) and 148.7 pcf (2,381.9 kg/m^3), respectively. The cylinders tested at 28 days had an average unconfined compressive strength and an average density of 6,003 psi (41.4 MPa) and 148.7 pcf (2,381.9 kg/m^3), respectively. The RSCR slabs were reinforced with conventional Grade 60 (413.7 MPa) steel.

Pressure and Impulse Histories

Reflected pressures were recorded at four corners and two side central locations around the slab. The BLS is designed to deliver approximately uniform pressure and observations have shown that the variations in pressures at individual locations were not significant. Table 1 shows the experimentally recorded average peak reflected pressures and impulses for the six slabs. These values reflect the average of the peak pressures recorded at each of the six pressure sensors on each slab. Figure 8 shows a schematic of the peak pressures experienced at each pressure sensor on slab HSCV1. The design pressures and impulses to be applied on the slab were arrived at based on initial SDOF calculations and experience. Figures 9 and 10 show the average reflected pressure and impulse histories for the slabs with 4 in. (101.6 mm) and 8 in. (203.2 mm) spacing respectively. From Table 1 it can be seen the peak pressure and impulse for two of the 4 in. slabs were 49.2-49.7 psi (339-343 kPa) and 997.6-1013.3 psi-msec (6878-6987 kPa-msec). To conserve resources and to gather additional information, when the

responses of two slabs were similar, it was decided to subject the third slab to a lower pressure-impulse history. Hence, the third slab had a peak pressure of 39.9 psi (275 kPa) and 773.9 psi-msec (5336 kPa-msec). However, two of the slabs with 8 in. (203.2 mm) spacing were subjected to an average peak pressure of 31.0-35.4 psi (214-244 kPa) and an average peak impulse of 511.6-576.1 psi-msec (3527-3972 kPa-msec), while the third slab had a higher average peak pressure of 41.1 psi (283 kPa) and a higher average impulse of 753.9 psi-msec (5198 kPa-msec).

SLAB #1
HSC - V1 - 4in.

Slab #1	
Driver Pressure	1150 psi
Driver Length	5.5 ft
HE/Air	0/100
Gap	2"

Gage	P (psi)	I (psi-msec)
P1	48.97	994.16
P2	54.72	1142.59
P3	52.39	998.72
P4	53.1	966.49
P5	53.48	978.36
P6	53.04	996.94
PD	53.2	986.16
PE	53.65	1042.8
Sum	422.55	8106.22
Avg	52.82	1013.28
S2		
S1		
	D (in)	
L1	3.89	
A1	3.97	

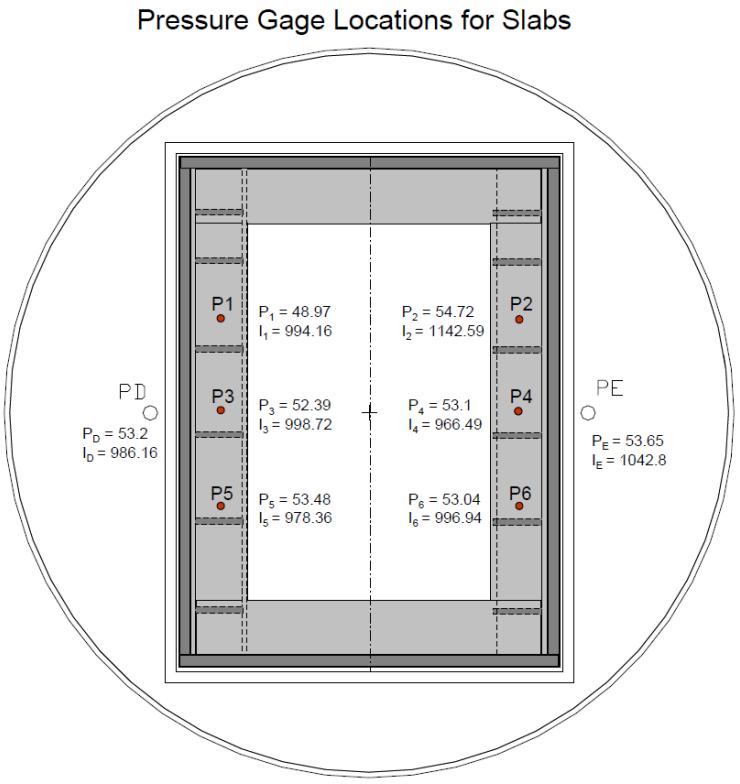

Figure 8- Peak Pressures Recorded at each Pressure Sensor on Slab HSCV1

In order to accurately show the effect of the varying pressure-time histories on the SDOF analyses, one high and one low pressure-time history were input into the SDOF Blast

Effects Design Spreadsheet (SBEDS) for both the 4 in. (101.6 mm) and 8 in. (203.2 mm) slabs to reflect this difference in subjected peak pressures and average impulses. These pressure-time histories are referred to as PH1, for the higher pressure-time history, and PH2, for the lower pressure-time history. For the 4 in. (101.6 mm) slabs PH1, shown in Table 2, refers to the pressure-time history for slab HSCV1 with an average peak pressure of 49.7 psi (342.7 kPa) and PH2, shown in Table 3, refers to the pressure-time history for slab HSCV3 with an average peak pressure of 39.9 psi (275.1 kPa). These pressure-time histories were chosen for the 4 in. (101.6 mm) reinforcement spacing slabs because the two higher pressure-time histories, for slabs HSCV1 and HSCV2, were relatively close (± 0.5 psi [± 3.45 kPa]) and, as a result, the higher of the two was chosen for PH1 and the remaining lower pressure-time history, for the slab HSCV3, was used for PH2. For the 8 in. (203.2 mm) slabs, PH1, shown in Table 4, refers to the pressure-time history for the slab HSCV4 with an average peak pressure of 41.1 psi (283.4 kPa) and PH2, shown in Table 5, refers to the pressure-time history for slab HSCV5 with an average peak pressure of 31.0 psi (213.7 kPa). These pressure-time histories were chosen for the 8 in. (203.2 mm) slabs because the two lower pressure-time histories, for slabs HSCV5 and HSCV6, were relatively close (± 4.4 psi [± 30.34 kPa]) and, as a result, the lower of the two was chosen for PH2 and the remaining higher pressure-time history, for the slab HSCV4, was used for PH1.

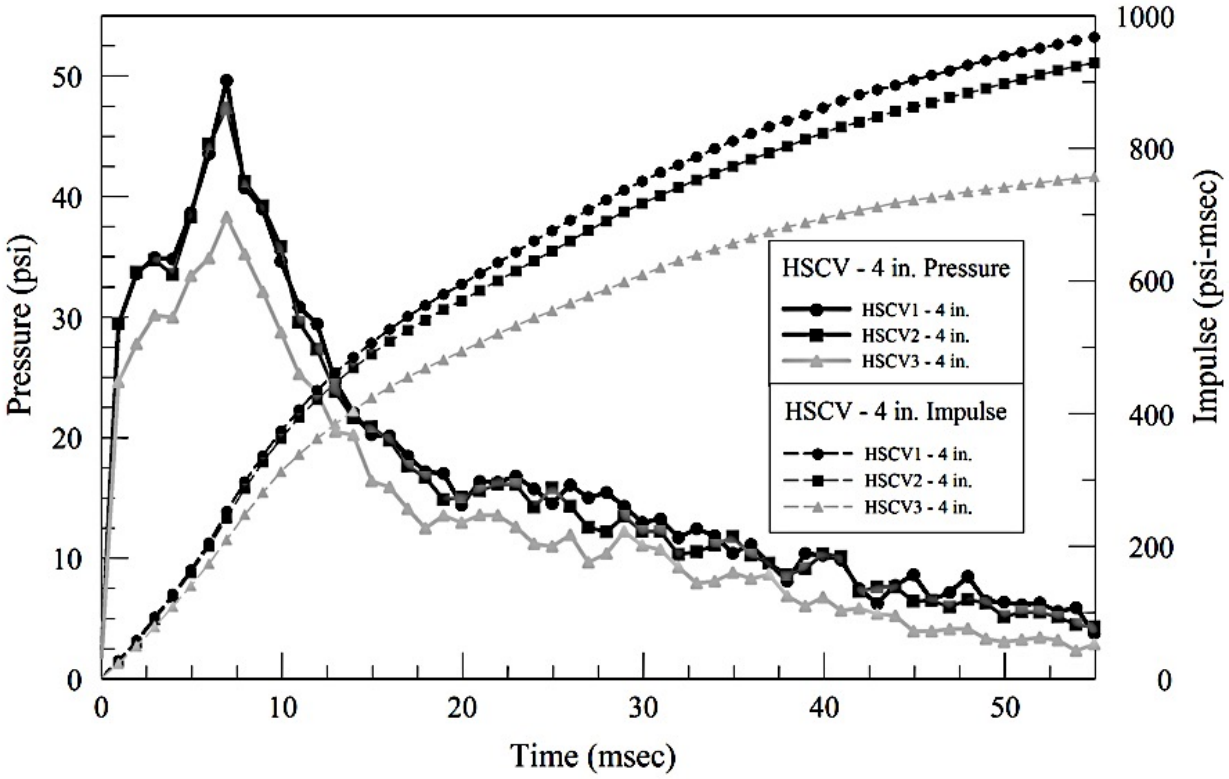

Figure 9- Input Reflected PI Curves for Slabs with 4 in. (101.6 mm) Bar Spacing (1 psi = 0.006895 MPa) (1 psi-msec = 6.895 kPa-msec)

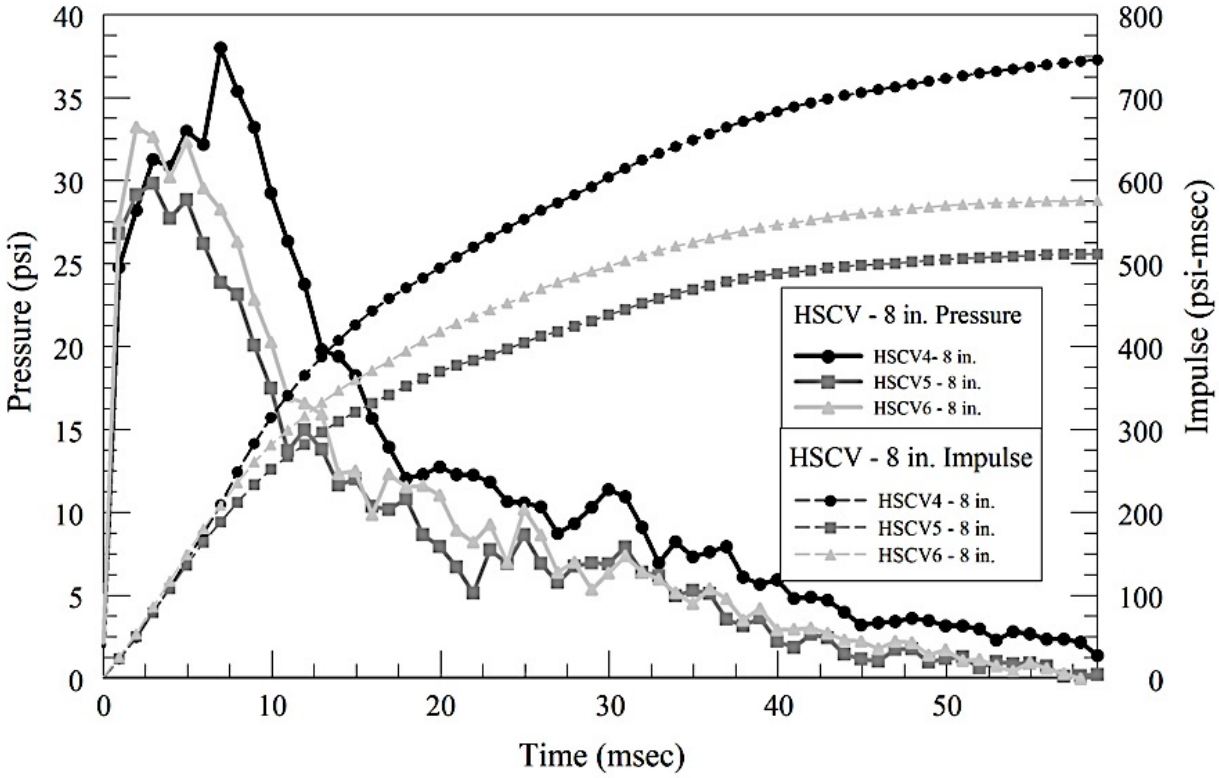

Figure 10- Input Reflected PI Curves for Slabs with 8 in. (203.2 mm) Bar Spacing (1 psi = 0.006895 MPa) (1 psi-msec = 6.895 KPa-msec)

Deflection Histories

Deflection was measured in two different ways. The first way of measuring deflection consisted of placing an accelerometer at the center of the panel's face, away from the blast side. The second way consisted of using a laser displacement sensor which pointed at a location very close to the accelerometer. The laser displacement sensor was used to record the displacement and the corresponding motion of the slab directly. The deflection from the accelerometer readings was derived by a double integration process. The accelerometer readings were recorded, but not discussed here since it is not a direct measurement of deflection. Figures 11 and 12 show the deflection readings from the laser device for the two sets of panels with 4 in. (101.6 mm) and 8 in. (203.2 mm) spacing respectively. The laser deflection is reported here as it clearly showed the residual deflection in the panel. It must be mentioned that some spikes were observed in the laser device readings as debris tends to fly off and intercept the laser light thereby artificially showing huge jumps in the deflection values. These jumps have been removed in the results reported. It can also be seen in Figure 11 that slab HSCV3 has a significantly lesser deflection compared to the other two slabs in the graph, noting it was subjected to a much lower pressure-impulse load as shown in Table 1. It should be noted that while HSCV2 was subjected to a higher pressure, it experienced a lower deflection than HSCV1 which was subjected to a lower pressure. This discrepancy was most likely caused by experimental construction defects or some other unforeseen reason. The SDOF model deflections obtained from the SBEDS analyses using the higher pressure-time history, PH1, and the lower pressure-time history, PH2, for both the 4 in. (101.6 mm) and 8 in. (203.2 mm) slabs, are discussed later in this thesis (and can be seen in Tables 9 and 10 in Chapter 6).

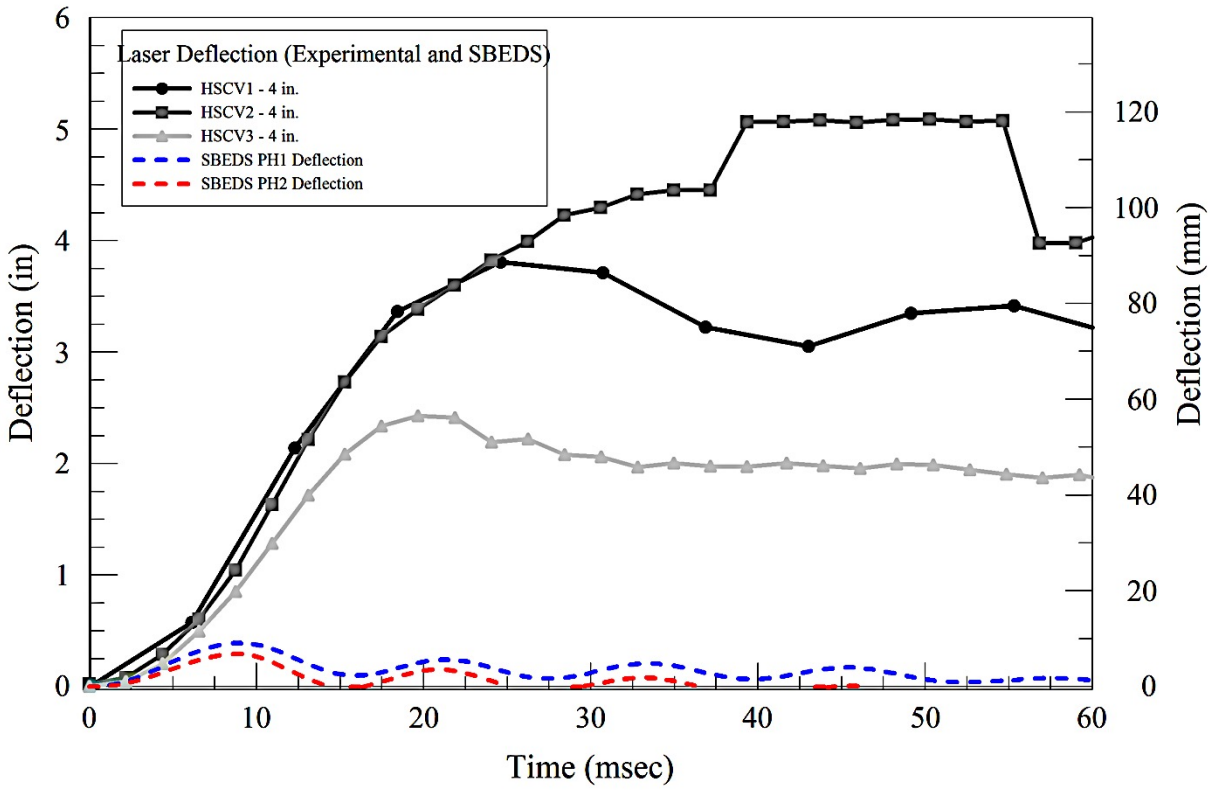

Figure 11- Experimental and Numerical (SBEDS) Deflection History for Slabs with 4 in. (101.6 mm) Bar Spacing (1 in. = 25.4 mm)

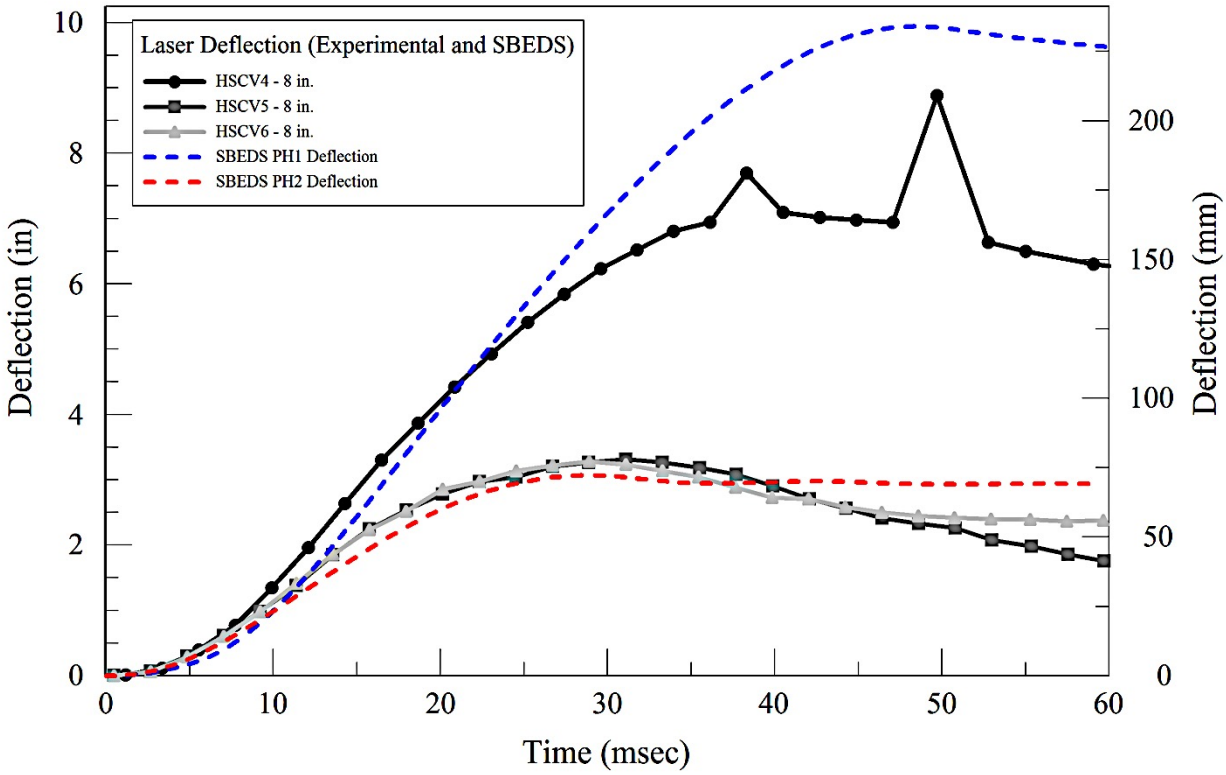

Figure 12- Experimental and Numerical (SBEDS) Deflection History for Slabs with 8 in. (203.2 mm) Bar Spacing (1 in. = 25.4 mm)

Table 1 also shows the peak deflection values and the residual deflection values of the panels. These deflection values have been converted to a damage value by stating deflection as a percentage of the slab span of 58 in. (1,473 mm) for comparison with PI curves discussed later in this thesis. The slab span is measured as the longitudinal (long) center-to-center distance between the simple HSS tube supports (Figure 7). As noted in the section on pressure histories the slabs with 4 in. (101.6 mm) spacing of longitudinal reinforcement bars were subjected to two sets of pressure and impulse values. From Table 1 it can be seen that for HSCV1 and HSCV2 slabs, with a higher PI, the peak deflections were 3.89 in. and 4.5 in. (99 mm and 114 mm) and the residual deflections were 2.02 in. (51 mm) and 3.5 in. (89 mm). The HSCV3 panel, with a lower PI input, had a peak deflection of 2.47 in. (63 mm) and a residual deflection of 1.37 in. (35 mm). For the panels with 8 in. (203.2 mm) longitudinal reinforcement spacing the peak deflection for HSCV5 and HSCV6 were very close ranging from 3.38-3.4 in. (86-87 mm) respectively, with residual deflections ranging from 1.53-1.9 in. (39-48 mm). HSCV4 experienced higher peak and residual deflections, 7.16 in. (183 mm) and 5.59 in. (142 mm), respectively. In this study the peak deflection parameter is defined as the peak deflection divided by the span and is expressed as a percentage and this parameter value has been found to range from 4.2 to 12.4 percent.

Table 1 – Recorded Experimental Data for Average Reflected Peak Pressure, Average Impulse, Peak Deflection, and Residual Deflection Values for all HSCV Slabs

	Average Peak Pressure, psi (kPa)	Average Impulse, psi-msec (kPa-msec)	Peak Deflection, in. (mm)	Peak Deflection as Percentage of Slab Span, %	Residual Deflection, in. (mm)	Residual Deflection as Percentage of Slab Span, %
HSCV1 - 4	49.7 (342.7)	1013.3 (6986.5)	3.89 (98.8)	6.7	2.02 (51.3)	3.5
HSCV2 - 4	49.2 (339.2)	997.6 (6878.2)	4.5 (114.3)	7.8	3.5 (88.9)	6.0
HSCV3 - 4	39.9(275.1)	773.9(5335.8)	2.47 (62.7)	4.2	1.37 (34.8)	2.4
HSCV4 -8	41.1 (283.4)	753.9 (5198.0)	7.16 (181.8)	12.4	5.59 (142.0)	9.6
HSCV5 - 8	31.0 (213.7)	511.6 (3527.4)	3.4 (86.4)	5.8	1.53 (38.9)	2.6
HSCV6 - 8	35.4 (244.1)	576.1 (3972.1)	3.38 (85.8)	5.8	1.9 (48.3)	3.3

Table 2 – Higher Pressure-Time History, PH1, for Slabs with 4 in. (101.6 mm) Bar Spacing

PH1 – 4 in.	
Time, ms	Pressure, psi (kPa)
0	11.43 (78.8)
2.65	49.67 (342.5)
10	34.84 (240.2)
20	14.31 (98.7)
30	12.77 (88.0)
40	10.75 (74.1)
50	6.06 (41.8)
60	0 (0)

Table 3 – Lower Pressure-Time History, PH2, for Slabs with 4 in. (101.6 mm) Bar Spacing

PH2 – 4 in.	
Time, ms	Pressure, psi (kPa)
0	6.72 (46.3)
2.65	39.93 (275.3)
10	28.19 (194.4)
20	12.86 (88.7)
30	11.18 (77.1)
40	6.52 (44.9)
50	3.28 (22.6)
60	0 (0)

Table 4 – Higher Pressure-Time History, PH1, for Slabs with 8 in. (203.2 mm) Bar Spacing

PH1 – 8 in.	
Time, ms	Pressure, psi (kPa)
0	6.74 (46.5)
7.49	41.13 (283.6)
10	28.49 (196.4)
20	12.55 (86.5)
30	11.51 (79.4)
40	5.94 (40.9)
50	2.68 (18.5)
60	0 (0)

Table 5 – Lower Pressure-Time History, PH2, for Slabs with 8 in. (203.2 mm) Bar Spacing

PH2 – 8 in.	
Time, ms	Pressure, psi (kPa)
0	6.12 (42.2)
2.65	31.00 (213.7)
10	17.48 (120.5)
20	7.87 (54.3)
30	6.94 (47.8)
40	2.30 (15.9)
50	1.26 (8.7)
60	0 (0)

Strain Histories

In order to achieve one of the experimental objectives, which was to determine experimental strain rates, two strain gages were placed on the tensile face of each panel along the longitudinal direction at quarter span locations and strain histories were recorded. The longitudinal direction was taken as the direction of the 58" (1.47 m) (long) slab span. Strain was recorded in this location because it is representative of the tensile strain along the span in the direction opposite the blast face. The quarter span locations were chosen to prevent the premature failure of the strain gages, because the cracks were expected to be primarily contained in the central region of the panel. Figure 7 shows where the strain gages were placed

at quarter span locations. The strain histories were used to compute and assess the strain rates experienced by the structure. Figure 13 shows the strain histories from the top and bottom strain gages (locations shown in Figure 7) of the 4 in. (101.6 mm) spaced longitudinal reinforcement panels (HSCV1, HSCV2, and HSCV3) and Figure 14 shows the same for panels with 8 in. (203.2 mm) longitudinal reinforcement spacing (HSCV4, HSCV5, and HSCV6). The following observations and conclusions can be drawn from these figures.

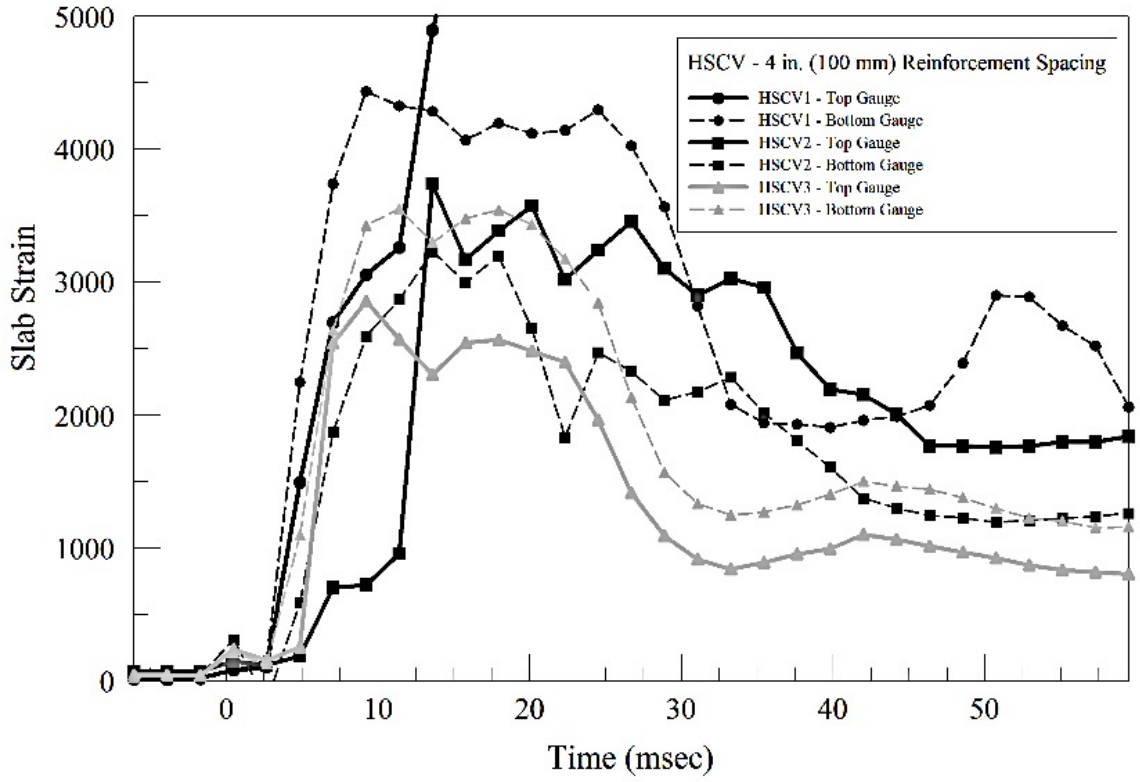

Figure 13- Strain History for Slabs with 4 in. (101.6 mm) Longitudinal Reinforcement Spacing

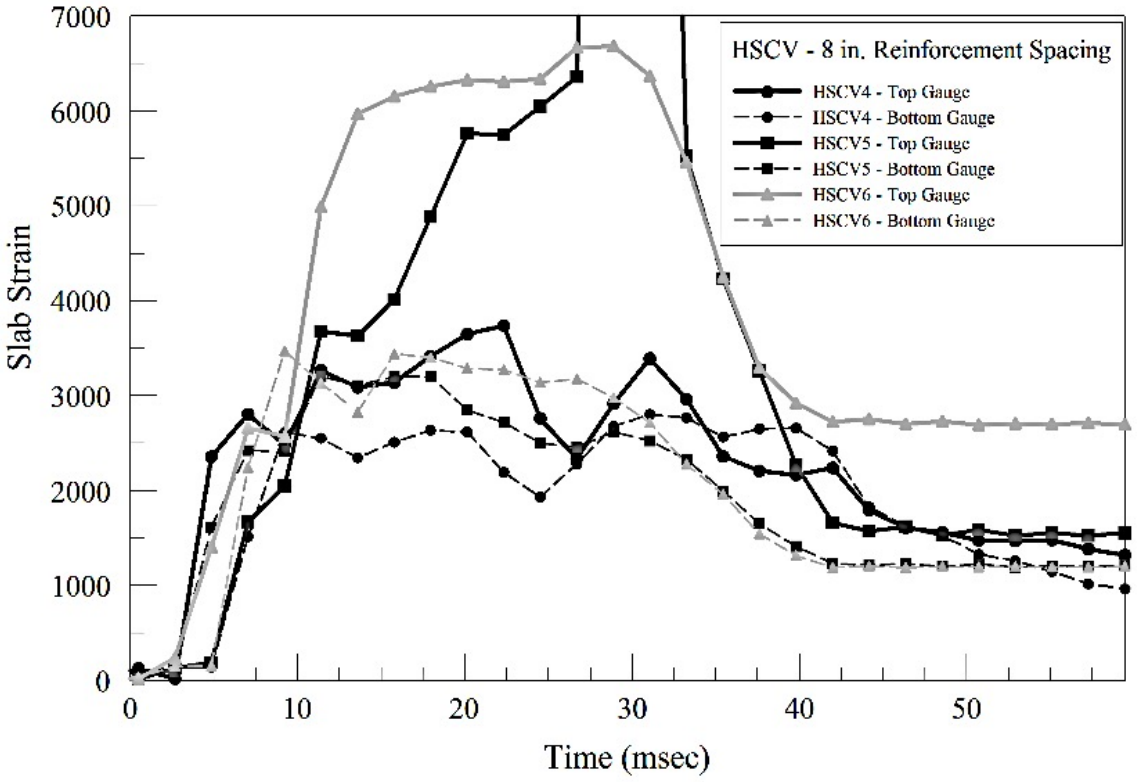

Figure 14- Strain History for Slabs with 8 in. (203.2 mm) Longitudinal Reinforcement Spacing

The member level strain rates have been determined using the strain history data. From all the curves in Figures 13 and 14 it can be seen that members experience a jump in strain between 5 and 10 milliseconds. Due to the possibility of high noise levels, no attempt is made here to quantify the strain rate experienced by the slab. Therefore the best interpretation of strain rate based on experimental data is provided in Figure 15 which shows a composite graph of the data points obtained from the twelve strain gages from the slabs HSCV1, HSCV2, HSCV3, HSCV4, HSCV5, and HSCV6. It can be qualitatively seen that the tensile strain rates can be as high as 7.5×10^6 /s while most of the data would indicate the strain rate in the range of 2.5×10^6 /s.

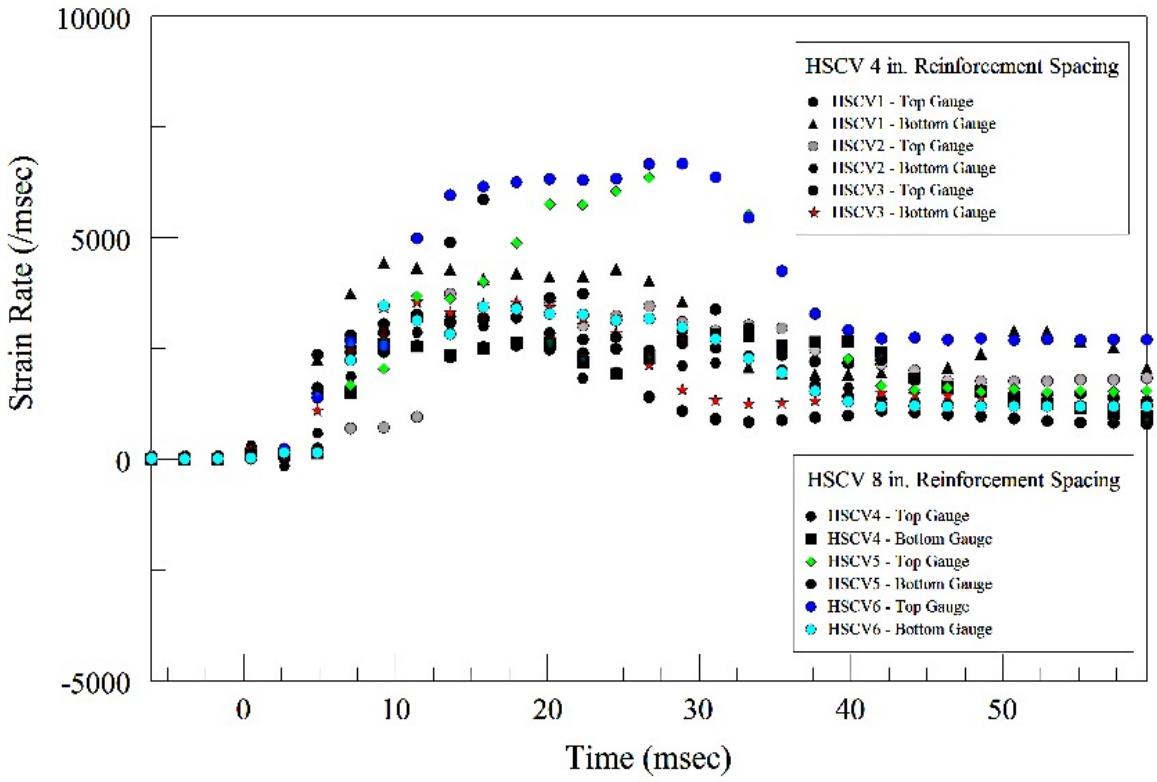

Figure 15- Qualitative Strain Rate Data for Slabs from Strain History Data

From Figure 13 it can be seen that the panels with a higher PI input (HSCV1 and HSCV2) had a peak tensile strain of around 3,700-5,000 με while HSCV3 had a lower peak strain of around 2,900 and 3,500 με in the top and bottom gages respectively. Figure 14 shows the strains from the two gages in slabs HSCV4, HSCV5, and HSCV6. The strains in these slabs showed a similar range of 3,700-6,700 με while one slab showed a very high value of around 20,000 με. These numbers are much higher than the static tensile failure strain in concrete. Since these gages where placed on the tension side, the higher recorded strains could be indicative of either a dynamic strength enhancement of concrete and/or formation of micro cracks, but not resulting in a failure of the strain gages. However, it is difficult to establish a quantitative structural dynamic increase factor from this data and further more specific tests are needed. Several authors have reported a material dynamic increase factor (16, 17). However, akin to defining ductility of the material, member, and structural levels in seismic behavior of structures, the observation from these experiments are indicative of a member level dynamic increase factor which combines the effect of both enhanced material strength and inertial effects due to the extreme dynamic loading.

SDOF and Experimental Pressure Impulse Comparison

This section describes the comparison of experimental results with a commonly used SDOF design method. SDOF models for structural components have been developed and used for the development of Pressure-Impulse (PI) curves (16, 18). Krauthammer et al. (12, 13) have used advanced SDOF approaches using analytical and numerical methods to study the effects of loading and material behavior on PI diagrams. Morison (19) presented a critical review of the application of SDOF analysis to one way and two way panels and concluded that they

appear to work well for one way panels, but could be deficient for two way panels. Several well developed programs exist to perform SDOF analysis for structural systems. One tool is a workbook called SDOF Blast Effects Design Spreadsheet (SBEDS), which was developed for the Protective Design Center for the United States Army Corps of Engineers (14). SBEDS is a component based tool used for the analysis and design of structures subjected to blast loading (20).

In order to develop PI diagrams for a slab using SDOF analysis, the determination of the final state of deformation of the structure is required. The response of the structure, subjected to a given blast load, is based on the durations of the blast load and the natural period of the structure (21). A SDOF model of a structure is constructed based on the dominant response mode of a structure which is responsible for the overall structural failure (22). SDOF modeling is simple, efficient, and represents the structural behavior based on the anticipated mode of response which determines the damage level of a structural system or structural element (5, 14).

However, SDOF analysis of a structure subjected to blast loading has its own disadvantages because damage may be governed by the local modes of the structure, especially when the loading is impulsive (2). Shi et al. (2008) (23) show that the SDOF model is not fully suitable to represent multi-failure modes of a structural component like a column that could collapse if shear failure precedes flexural failure. In addition, SDOF models assume either rigid plastic or bilinear elastic-plastic-rigid material idealization and may neglect strain hardening effects in the analysis, thereby not accurately reflecting the true behavior of the structure (23).

The natural time period of a structure is an important component of an SDOF analysis. The fundamental period for an elastic slab simply supported and subjected to a uniformly

distributed force is computed. With a modulus of elasticity of concrete of 48,133 MPa for a concrete compressive strength of 103 MPa and assuming that the effective moment of inertia of the slab to be 70 percent of its gross moment of inertia, $I_{eff} = 5.28 \times 10^7$ mm^4 the stiffness is calculated to be 61,109 N/mm (15). The mass of the slab is 800 kg from which the fundamental period is calculated to be 23 ms. The values reported from SBEDS are 12.2 ms and 13.5 ms for the 4 in. (101.6 mm) and 8 in. (203.2 mm) 9.5 mm diameter reinforcement bar spacing slabs respectively. The high and low pressure-time histories discussed earlier, PH1 and PH2, were input into SBEDS for both the 4 in. (101.6 mm) and 8 in. (203.2 mm) slabs and 4 PI curves were generated. The SBEDS generated PI curves for PH1 and PH2 for the 4 in. (101.6 mm) slabs are shown in Figures 16 and 17, respectively. Similarly, the SBEDS generated PI curves for PH1 and PH2 are shown in Figures 18 and 19, respectively.

Figures 16 through 19 also show the comparison of the experimental data points with the PI curves generated using the SDOF program SBEDS. The PI curves shown by broken lines represent the curves a designer would currently use, when slabs of the configuration used in testing are proposed. The levels of protection (LOP) are defined per UFC 4-010-01 (24) and incorporated in SBEDS. The levels of protection are a) Very low level of protection (VLOP), b) Low level of protection (LLOP) and c) Medium/high level of protection (MHLOP). Two criteria are used by UFC 4-010-01 for defining the levels of protection. They are θ (slab end rotation) and μ (slab ductility). In blast design, the peak deflection values are often chosen as a measure for the LOP. The metrics of LOP for structural elements defined in the ASCE Standard 59-11 (25) are based on the ductility ratio and rotation at the support. The ductility ratio is defined as the ratio of the maximum deflection to yield deflection of the member while,

the support rotation is the rotation at the supports when the maximum dynamic deflection is reached.

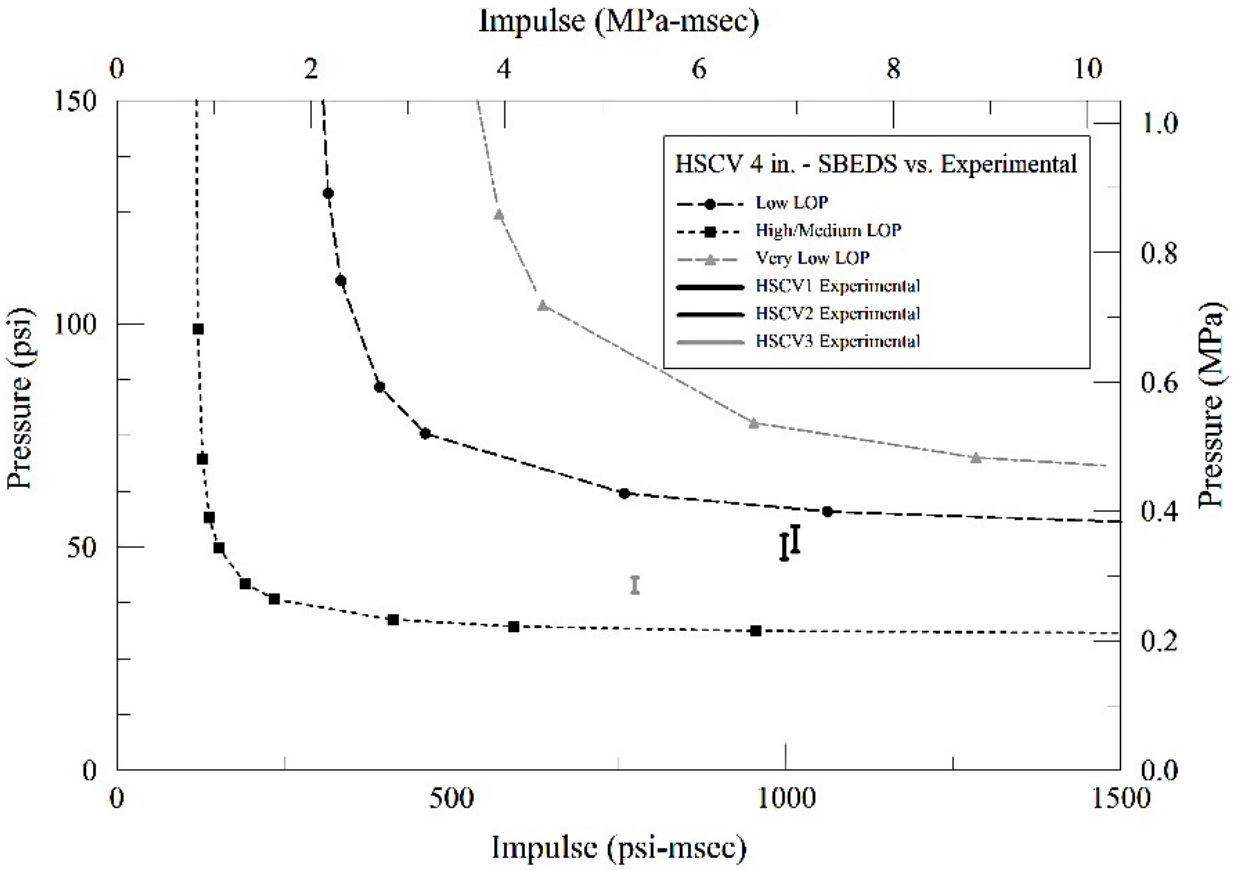

Figure 16- Input PI Curves for Slabs with 4 in. (101.6 mm) Bar Spacing (1 psi = 0.006895 MPa) (1 psi-msec = 0.006895 MPa-msec) and SBEDS PH1 Input

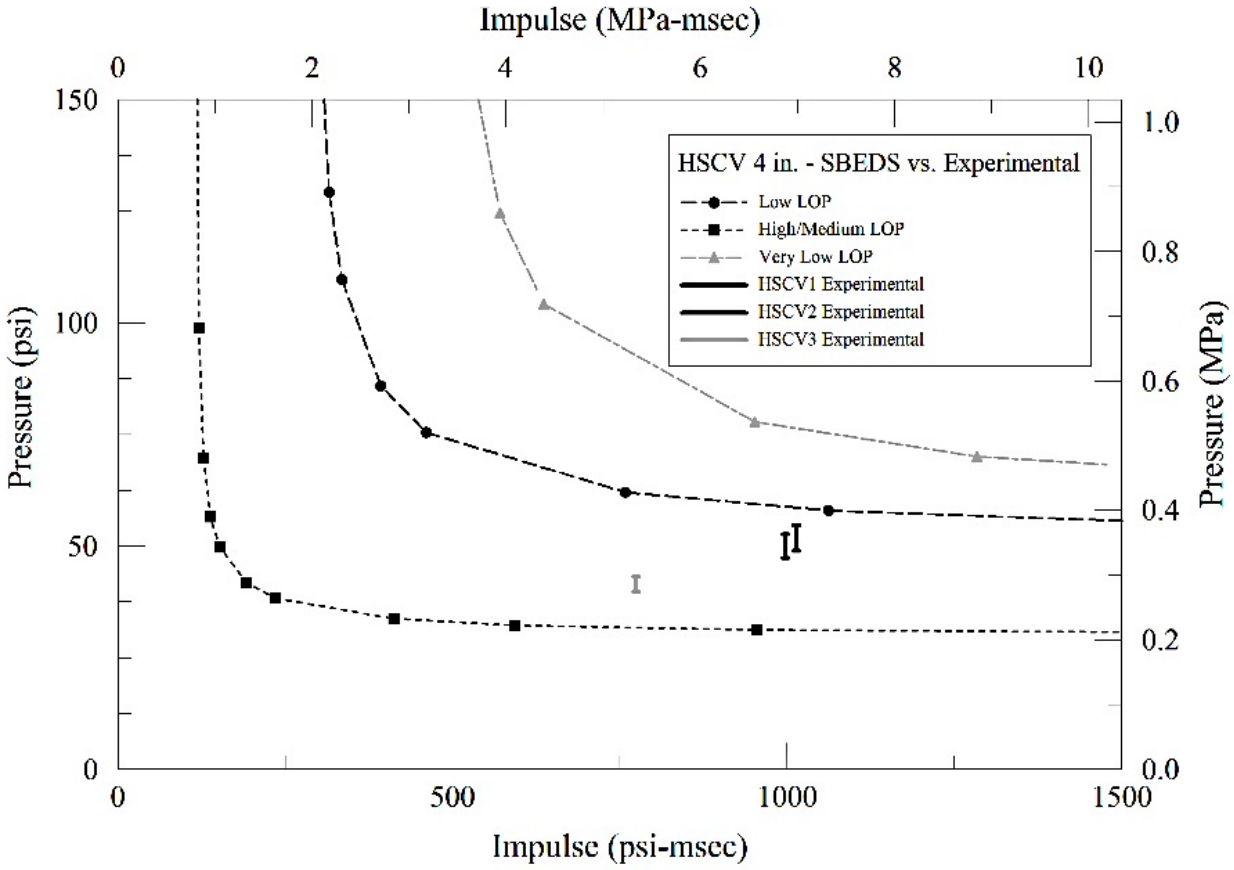

Figure 17- Input PI Curves for Slabs with 4 in. (101.6 mm) Bar Spacing (1 psi = 0.006895 MPa) (1 psi-msec = 0.006895 MPa-msec) and SBEDS PH2 Input

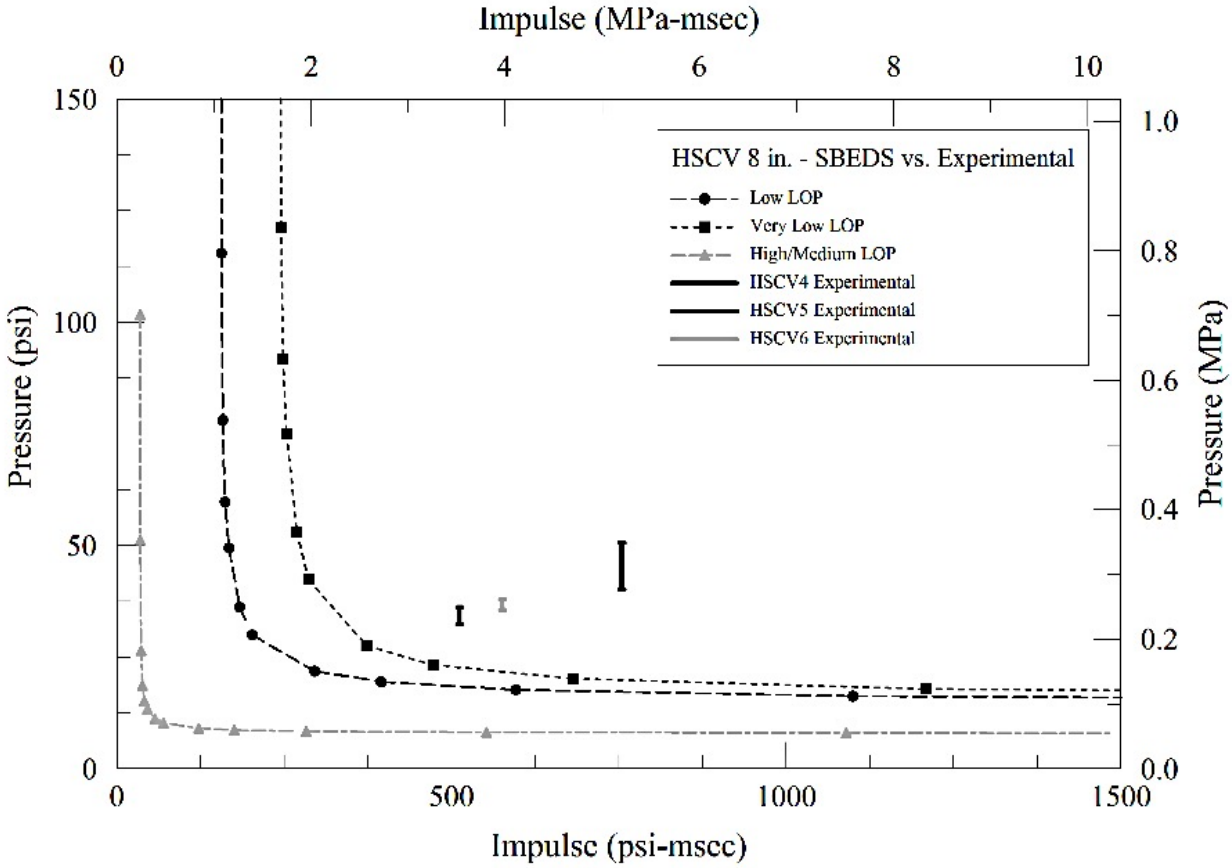

Figure 18- Input PI Curves for Slabs with 8 in. (203.2 mm) Bar Spacing (1 psi = 0.006895 MPa) (1 psi-msec = 0.006895 MPa-msec) and SBEDS PH1 Input

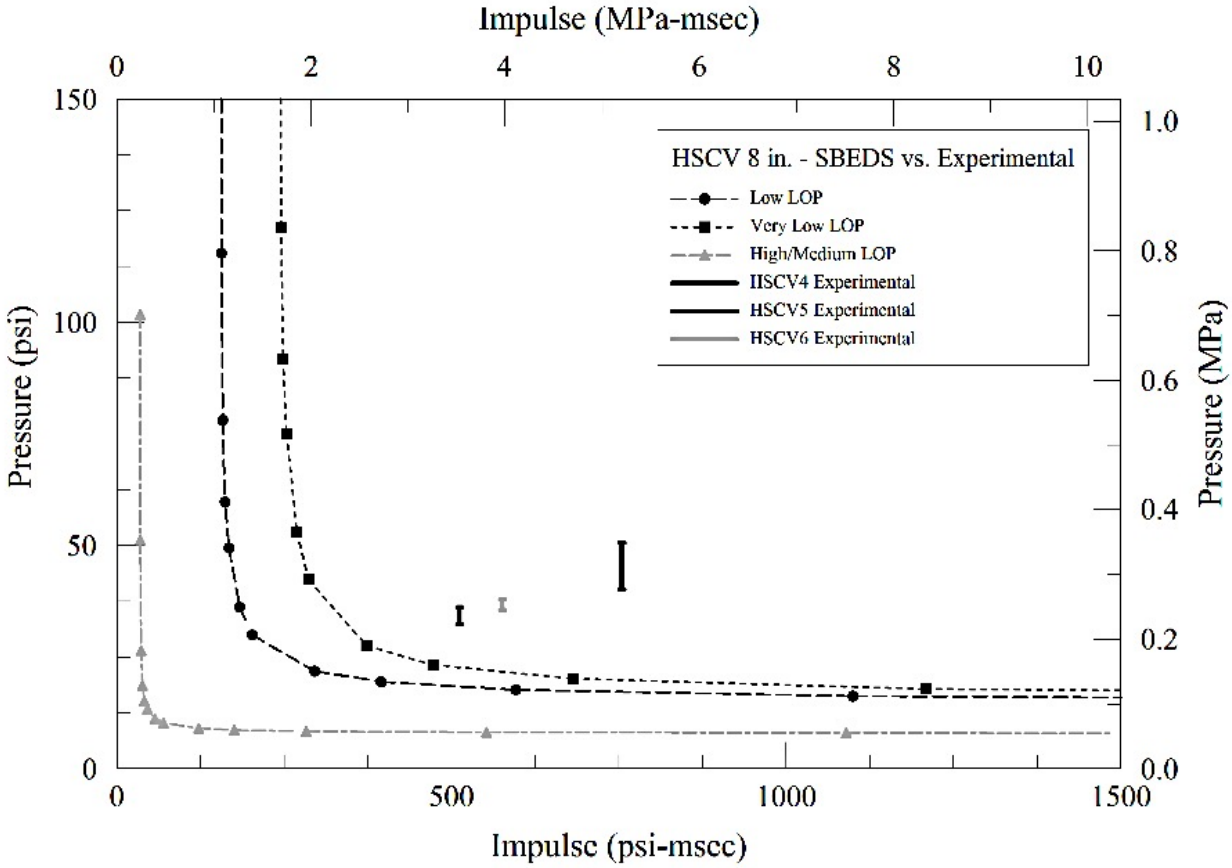

Figure 19- Input PI Curves for Slabs with 8 in. (203.2 mm) Bar Spacing (1 psi = 0.006895 MPa) (1 psi-msec = 0.006895 MPa-msec) and SBEDS PH2 Input

For the VLOP and LLOP criteria, the slab end rotation values are specified to be 5 degrees and 2 degrees, respectively. For MHLOP, there is no specified slab end rotation, but the ductility value is defined to be 1. These LOP criteria correspond to a peak central deflection of 1.01 and 2.54 inches (26 and 65 mm) for VLOP and LLOP respectively. For MHLOP the ductility value depends not only on the slab geometry, but also on the reinforcement details. For #3 bars at 4 in. (101.6 mm) c/c the MHLOP criterion corresponds to a peak central displacement of 0.31 in. (7.9 mm) and for #3 bars at 8 in. (203.2 mm) c/c the peak displacement value is 0.1 in. (2.5 mm). These peak central displacements are the same for PH1 and PH2 for both sets of slabs. The equivalent deflection values are taken from SBEDS as the maximum deflection for the given level of protection.

Also, shown in Figures 16 through 19 are experimental PI data for each of the three slabs. Each experimental data point shows the high/low values of pressure experienced by the six pressure gages in the slab for the average impulse on the slab. Table 1 shows the average peak reflected pressure, average impulse, peak and residual deflection, and the corresponding damage values for each of the tests. The damage values are calculated by dividing the peak deflection by the span of 58 in. (1473 mm) and reporting it as a percentage.

The following observations are made from Figures 16 and 17. For the 4 in. (101.6 mm) slab, the design curve corresponding to the MHLOP is conservative compared to the experimental damage levels while the design curves corresponding to the VLOP and LLOP are higher and fall above the experimental damage levels experienced by all three slabs. In other words, the design PI values per SBEDS for MHLOP are lower than what the slabs can actually withstand while the design PI values per SBEDS for VLOP and LLOP are higher than what the slabs can actually withstand. From the observed experimental PI values, it can be seen

that HSCV1 and HSCV2 were subjected to higher pressure and impulse combinations than HSCV3 and withstood higher values than that predicted by the curve corresponding to the MHLOP. The lower pressure and impulse combination subjected to HSCV3 is below those of HSCV1 and HSCV2 and all three fall below the lines corresponding to the design very low and low LOP curves and are above the line corresponding to the design medium/high LOP curve.

The following observations are made from Figures 18 and 19. The design curves corresponding to the various LOP for the 8 in. (203.2 mm) slabs are also conservative compared to the experimental damage levels, shown in Figure 17, and the design PI values are much lower than those that the slabs can actually withstand. For the 8 in. (203.2 mm) slabs it can be seen that the design curves predict that the slabs can withstand much lower PI values, even at high/medium LOP, compared to the pressure and impulse combinations subjected to HSCV4, HSCV5, and HSCV6. All of the pressure and impulse combinations for the 8 in. (203.2 mm) slabs fall above the line corresponding to the design low LOP curve. A conclusion can be made by taking into consideration the much lower PI values predicted by the design curves compared to the subjected pressure and impulse combinations for the 8 in. (203.2 mm) slabs and the higher PI values predicted by the design curves compared to the subjected pressure and impulse combinations for the 4 in. (101.6 mm) slabs. This conclusion is that there is sufficient conservatism built into the design curves developed using SBEDS for the 8 in. (203.2 mm) slabs and that there is modest conservatism built into the design curves using SBEDS for the 4 in. (101.6 mm) slabs.

Experimental Deflection and Dynamic Resistance Curves and SBEDS Comparison

Resistance curves are commonly used in the design of members subjected to blast loading. Fallah and Louca (26) have outlined the derivation of an elasto-plastic resistance curve for a SDOF system. Static resistance curves can also be determined experimentally using various methods such as the water tank tests or they can be determined numerically from programs such as SBEDS. In this study an attempt is made to characterize the actual dynamic behavior of the slab by plotting the force on the slab, which is determined using the pressure and surface area of the slab, against the deflection.

Figure 20 shows the experimental dynamic resistance curve and the corresponding PH1 and PH2 curves generated by SBEDS for the 4 in. (101.6 mm) set of slabs. From the plot, yielding points at (2.03 mm, 267.9 kN), (1.52 mm, 283.5 kN), and (1.52 mm, 239.8 kN) can be observed for HSCV1, HSCV2, and HSCV3, respectively. Examining the plot points (20.07 mm, 357.3 kN), (14.48 mm, 371.1 kN), and (14.73 mm, 304.6 kN) for HSCV1, HSCV2, and HSCV3, respectively, it can be noted that the three 4 in. (101.6 mm) slabs developed considerable post-yield strength with some ductility. The slope of the plot indicates that the 4 in. (101.6 mm) slabs experienced considerable softening. Looking at the plot, it can be seen that the peak resistance force and maximum displacement predicted by SBEDS for the 4 in. (101.6 mm) slabs were (59.5 kN, 9.91 mm) and (56.4 kN, 7.37 mm) for PH1 and PH2, respectively. These values do not compare well with the observed experimental data.

Figure 21 shows the experimental dynamic resistance curve and the corresponding PH1 and PH2 curves generated by SBEDS for the 8 in. (203.2 mm) slabs. From the plot, yielding points at (15 mm, 289.5 kN), (1.02 mm, 219.2 kN) and (1.02 mm, 242.7 kN) can be observed for HSCV4, HSCV5, and HSCV6, respectively. Post-yielding behavior can be seen at (16.51

mm, 308.6 kN), (2.03 mm, 236.7 kN), and (1.52 mm, 272.9 kN) for HSCV4, HSCV5, and HSCV6, respectively. The peak resistance force and maximum displacement predicted by SBEDS for the 8 in. (203.2 mm) slabs were (15.9 kN, 252.5 mm) and (15.9 kN, 77.98 mm) for PH1 and PH2, respectively. The peak resistance for the 8 in. (203.2 mm) slabs does not compare very well with the observed experimental data while the maximum displacement compares fairly well.

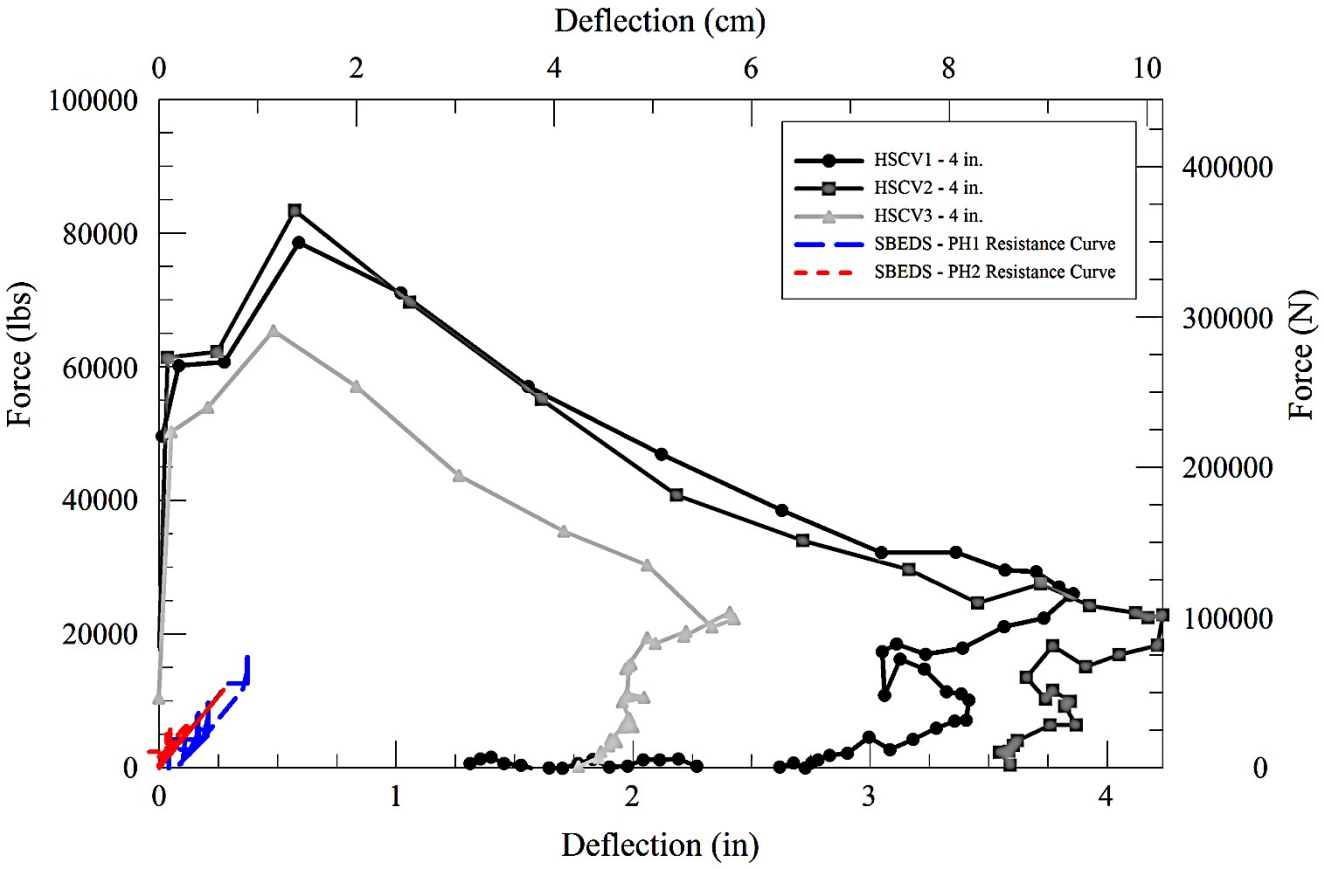

Figure 20- Dynamic Resistance Curves for Slabs with 4 in. (101.6 mm) Bar Spacing (1 in. = 2.54 cm) (1 lb = 4.448 N)

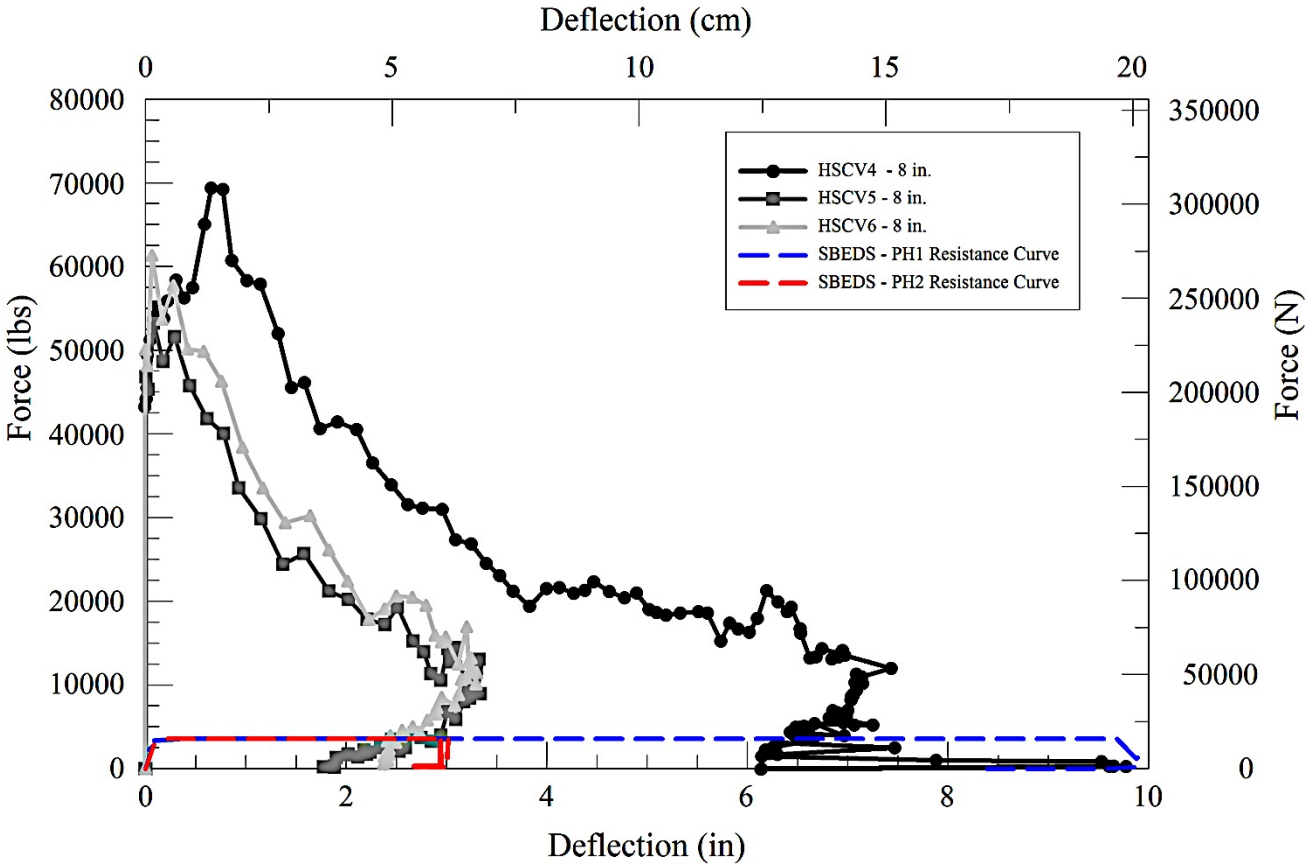

Figure 21- Dynamic Resistance Curves for Slabs with 8 in. (203.2 mm) Bar Spacing (1 in. = 2.54 cm) (1 lb = 4.448 N)

The following observations are made from Figures 20 and 21. The 4 in. (101.6 mm) slabs were able to develop higher post yield strengths and exhibited higher ductility than the 8 in. (203.2 mm) slabs. Observing the slopes of the two plots, it can be seen that the 4 in. (101.6 mm) slabs experienced further softening compared to the 8 in. (203.2 mm) slabs. The observed experimental dynamic resistance for both the 4 in. (101.6 mm) slabs and the 8 in. (203.2 mm) slabs exhibited much lower values than those predicted by SBEDS. In addition, the peak deflection predicted by SBEDS for the 8 in. (203.2 mm) slabs was comparable to those observed experimentally while the peak deflection predicted by SBEDS for the 4 in. (101.6 mm) was much lower than those observed experimentally. These observations indicate that spacing restrictions are critical in the design of slabs subjected to blast loading.

CHAPTER 6

ADDITIONAL SDOF MODEL MAXIMUM DEFLECTION STUDY

Several different analyses were performed using SBEDS to additionally study how SDOF models predict blast behavior of high-strength concrete slabs, reinforced with Vanadium steel. In the first analysis, the actual experimental pressure time histories for each of the 4 in. (101.6 mm) and 8 in. (203.2 mm) center-to-center reinforcement spacing slabs were entered into SBEDS. A separate SDOF model was created for each slab with its corresponding actual experimental pressure-time history, and the maximum numerical deflection obtained from SBEDS was then compared to the actual experimental maximum deflection. For the second analysis, the pressure time histories described previously, PH1 and PH2, for the 4 in. (101.6 mm) and 8 in. (203.2 mm) were entered into SBEDS. Four individual SDOF models were developed and the maximum numerical deflections obtained from SBEDS were compared to the maximum actual experimental deflection values. The PI design curves and resistance values obtained from this analysis were discussed previously in this thesis.

Individual Pressure-Time Histories

Following the slab experiments, the experimental maximum pressures and the experimental times of maximum pressure for HSCV1, HSCV2, HSCV3, HSCV4, HSCV5, and HSCV6 were entered into SBEDS. In addition, the pressures at 0 ms, 10 ms, 20 ms, 30 ms, 40 ms, 50 ms, and 60 ms were entered into SBEDS for HSCV1, HSCV2, HSCV3, HSCV4, HSCV5, and HSCV 6. These pressure and time histories were obtained from the experimental data for each slab and are summarized in Tables 6 and 7. A separate SBEDS analysis was ran

for each slab and the maximum numerical deflection value obtained was compared to the maximum experimental deflection values. The maximum experimental deflection values and the maximum numerical deflection values obtained from SBEDS for each slab are shown in Table 8.

Table 6 – Actual Experimental Pressure-Time Histories Input into SBEDS for Slabs with 4 in. (101.6 mm) Bar Spacing

HSCV1		HSCV2		HSCV3	
Time, ms	Pressure, psi (kPa)	Time, ms	Pressure, psi (kPa)	Time, ms	Pressure, psi (kPa)
0	11.431 (78.8)	0	4.357 (30.2)	0	6.724 (46.4)
6.926	49.671 (342.5)	6.575	49.183 (339.1)	7.212	39.928 (275.3)
10	34.840 (240.2)	10	35.392 (244.0)	10	28.195 (194.4)
20	14.309 (98.7)	20	15.895 (109.6)	20	12.860 (88.7)
30	12.775 (88.1)	30	11.818 (81.5)	30	11.177 (77.1)
40	10.748 (74.1)	40	10.170 (70.1)	40	6.518 (45.6)
50	6.059 (41.8)	50	5.563 (38.4)	50	3.283 (22.6)
60	0 (0)	60	0 (0)	60	0 (0)

Table 7 – Actual Experimental Pressure-Time Histories Input into SBEDS for Slabs with 8 in. (203.2 mm) Bar Spacing

HSCV4		HSCV5		HSCV6	
Time (ms)	Pressure (psi)	Time (ms)	Pressure (psi)	Time (ms)	Pressure (psi)
0	6.743 (46.5)	0	6.118 (42.2)	0	0.730 (5.0)
7.487	41.128 (283.6)	2.649	31.004 (213.8)	2.617	35.399 (244.1)
10	28.491 (196.4)	10	17.485 (120.5)	10	20.299 (140.0)
20	12.546 (86.5)	20	7.873 (54.3)	20	10.755 (74.1)
30	11.514 (79.4)	30	6.943 (47.9)	30	6.237 (43.0)
40	5.941 (41.0)	40	2.296 (15.8)	40	2.916 (20.1)
50	2.677 (18.5)	50	1.265 (8.7)	50	1.504 (10.4)
60	0 (0)	60	0 (0)	60	0 (0)

Table 8 – Actual Experimental Maximum Deflection vs. Numerical Maximum Deflection for all Slabs

		Maximum Deflection, x_{max}, in. (mm)
HSCV1	Experimental	3.89 (98.8)
	SBEDS	0.39 (9.9)
HSCV2	Experimental	4.50 (114.3)
	SBEDS	0.41 (10.4)
HSCV3	Experimental	2.47 (62.7)
	SBEDS	0.29 (7.4)
HSCV4	Experimental	7.16 (181.9)
	SBEDS	9.94 (252.5)
HSCV5	Experimental	3.40 (86.4)
	SBEDS	3.07 (78.0)
HSCV6	Experimental	3.38 (85.8)
	SBEDS	5.26 (133.6)

Comparing the maximum experimental deflection values, to the maximum numerical deflection values obtained from SBEDS, using the actual pressure time histories experienced by each respective slab, several conclusions can be made. The maximum numerical deflection values obtained from SBEDS for HSCV1, HSCV2, and HSCV3 were 90% smaller, 91% smaller, and 88% smaller, respectively, than the actual maximum experimental deflection values experienced by the slabs. The maximum numerical deflection values obtained from SBEDS for HSCV4, HSCV5, and HSCV6 were 39% larger, 10% smaller, and 56% larger,

respectively, than the maximum experimental deflection values experienced by the slabs. Looking at the smaller percentage differences, it can be seen that SBEDS produced more accurate maximum numerical deflections for the 8 in. (203.2 mm) slabs than for the 4 in. (101.6 mm) slabs. SBEDS also produced larger deflection values, sometimes even in excess of the experimental deflection, for the 8 in. (203.2 mm) slabs vs. the 4 in. (101.6 mm) slabs. Thus, for actual pressure vs. time histories, SBEDS produces less accurate yet more conservative deflection values for the 4 in. (101.6 mm) slabs and more accurate yet less conservative deflection values for the 8 in. (203.2 mm) slabs. In other words, SBEDS predicted an average maximum deflection that is 90% less than what the 4 in. (101.6 mm) slabs can actually withstand and 28% more than what the 8 in. (203.2 mm) slabs can actually withstand.

Higher and Lower Pressure-Time History Analysis

Continuing the numerical analysis, the higher and lower pressure-time histories, PH1 and PH2, for the 4 in. (101.6 mm) slabs were gathered. The maximum pressures and times of maximum pressure for PH1 and PH2 were entered into SBEDS. Similarly, the pressures at 0 ms, 10 ms, 20 ms, 30 ms, 40 ms, 50 ms, and 60 ms for PH1 and PH2 were also entered into SBEDS. These pressure and time values can be observed in Tables 2 and 3. The same procedure was done for the maximum pressure, time of maximum pressure, and pressures at 0 ms, 10 ms, 20 ms, 30 ms, 40 ms, 50 ms, and 60 ms for PH1 and PH2 for the 8 in. (203.2 mm) slabs. These pressure and time values can be seen in Tables 4 and 5. These values were also input into SBEDS to obtain the pressure-impulse design curves and dynamic resistance curves discussed previously. The maximum deflections obtained from the SBEDS analysis for the 4 in. (101.6 mm) slabs were 0.39 in. (9.91 mm) and 0.29 in. (7.37 mm) for PH1 and PH2,

respectively. The maximum numerical deflections obtained from the SBEDS analysis for the 8 in. (203.2 mm) slabs were 9.94 in. (252.5 mm) and 3.07 in. (77.98 mm) for PH1 and PH2, respectively.

As discussed previously, for the 4 in. (101.6 mm) slabs, PH1 corresponds to the pressure-time history for HSCV1 and PH2 corresponds to the pressure-time history for HSCV3. The maximum experimental deflections for HSCV1 and HSCV3 were 3.89 in. (98.81 mm) and 2.47 in. (62.74 mm), respectively. When comparing these values to the value for the 4 in. (101.6 mm) slabs predicted by SBEDS using PH1 and PH2, it can be seen that the maximum numerical deflection is 90% smaller for PH1 and 88% smaller for PH2 than the maximum deflection values observed experimentally for slabs HSCV1 and HSCV3, respectively. This same conclusion was made in the previous individual pressure-history section for HSCV1 and HSCV3 and their corresponding maximum deflections are shown in Table 8. For the sake of clarification regarding the deflection versus time plot in Figure 11, the maximum experimental and numerical deflection values are shown together in Table 9.

Table 9 – Maximum Deflection Values Observed Experimentally and from PH1 and PH2 SBEDS Analyses for Slabs with 4 in. (101.6 mm) Bar Spacing

	HSCV 4 in. Maximum Deflection, x_{max}, in. (mm)
Experimental – HSCV1	3.89 (98.8)
SBEDS – PH1	0.39 (9.9)
Experimental – HSCV3	2.47 (62.7)
SBEDS – PH2	0.29 (7.4)

As discussed previously, for the 8 in. (203.2 mm) slabs, PH1 corresponds to the pressure-time history for HSCV4 and PH2 corresponds to the pressure-time history for HSCV5. The maximum experimental deflections for HSCV4 and HSCV5 were 7.16 in. (181.9 mm) and 3.4 in. (86.36 mm), respectively. When comparing these values to the value for the 8 in. (203.2 mm) slabs predicted by SBEDS using PH1 and PH2, it can be seen that the maximum numerical deflection is 39% larger for PH1 and 10% smaller for PH2 than the maximum deflection values observed experimentally for slabs HSCV1 and HSCV3, respectively. This same conclusion was made in the previous individual pressure-history section for HSCV4 and HSCV5 and their corresponding maximum deflections are shown in Table 8. For the sake of clarification regarding the deflection versus time plot in Figure 12, the maximum experimental and numerical deflection values are shown together in Table 10.

Table 10 – Maximum Deflection Values Observed Experimentally and from PH1 and PH2 SBEDS Analyses for Slabs with 8 in. (203.2 mm) Bar Spacing

	HSCV 8 in. Maximum Deflection, x_{max}, in. (mm)
Experimental – HSCV4	7.16 (181.9)
SBEDS – PH1	9.94 (252.5)
Experimental – HSCV5	3.40 (86.4)
SBEDS – PH2	3.07 (78.0)

Maximum deflection plots, showing the maximum experimental deflection and the maximum numerical deflection from SBEDS using the experimental pressure time histories for the 4 in. (101.6 mm) and 8 in. (203.2 mm) center-to-center reinforcement spacing slabs can be seen in Figures 22 to 27.

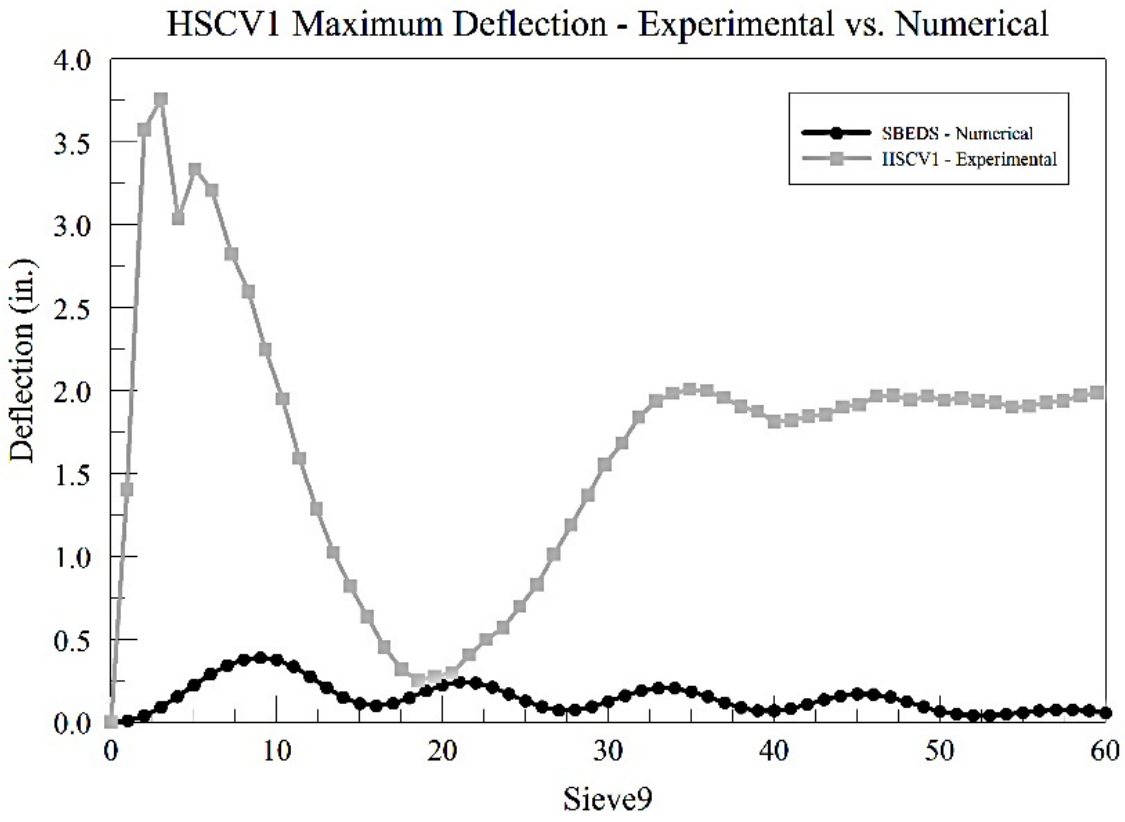

Figure 22- Maximum Experimental Deflection vs. SBEDS Actual Pressure-Time History Maximum Numerical Deflection for Slab HSCV1

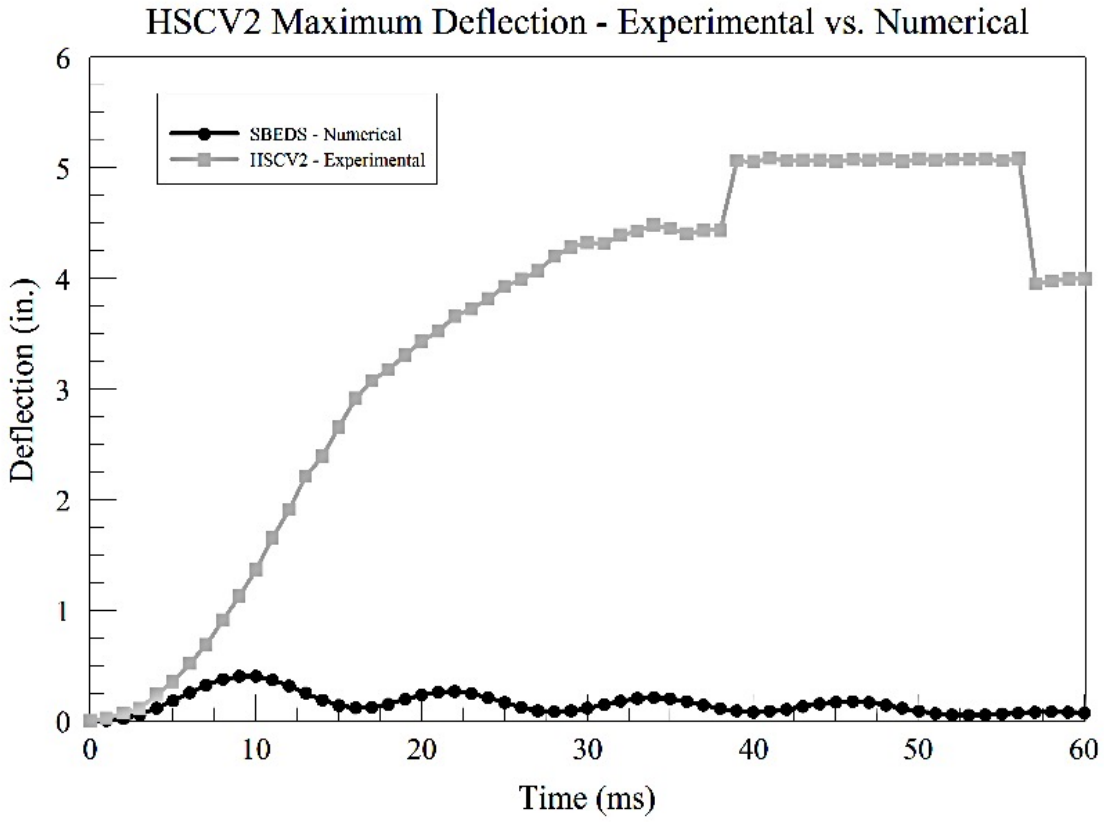

Figure 23- Maximum Experimental Deflection vs. SBEDS Actual Pressure-Time History Maximum Numerical Deflection for Slab HSCV2

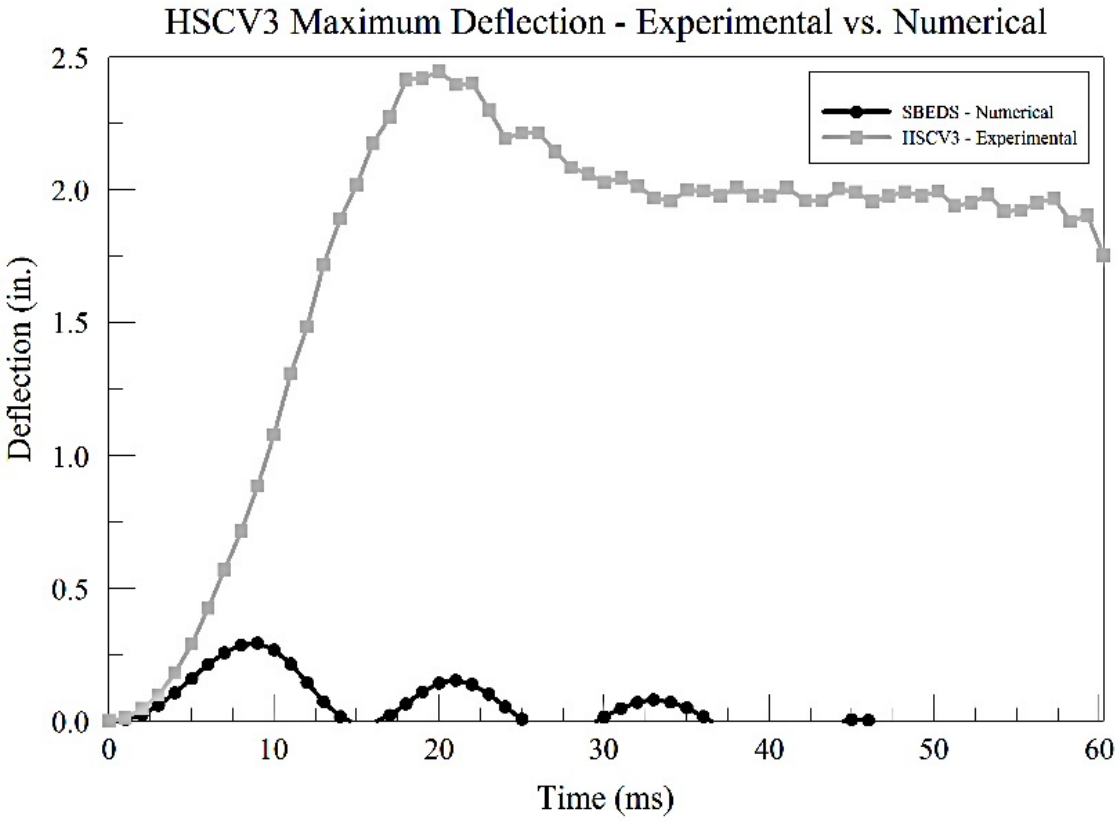

Figure 24- Maximum Experimental Deflection vs. SBEDS Actual Pressure-Time History Maximum Numerical Deflection for Slab HSCV3

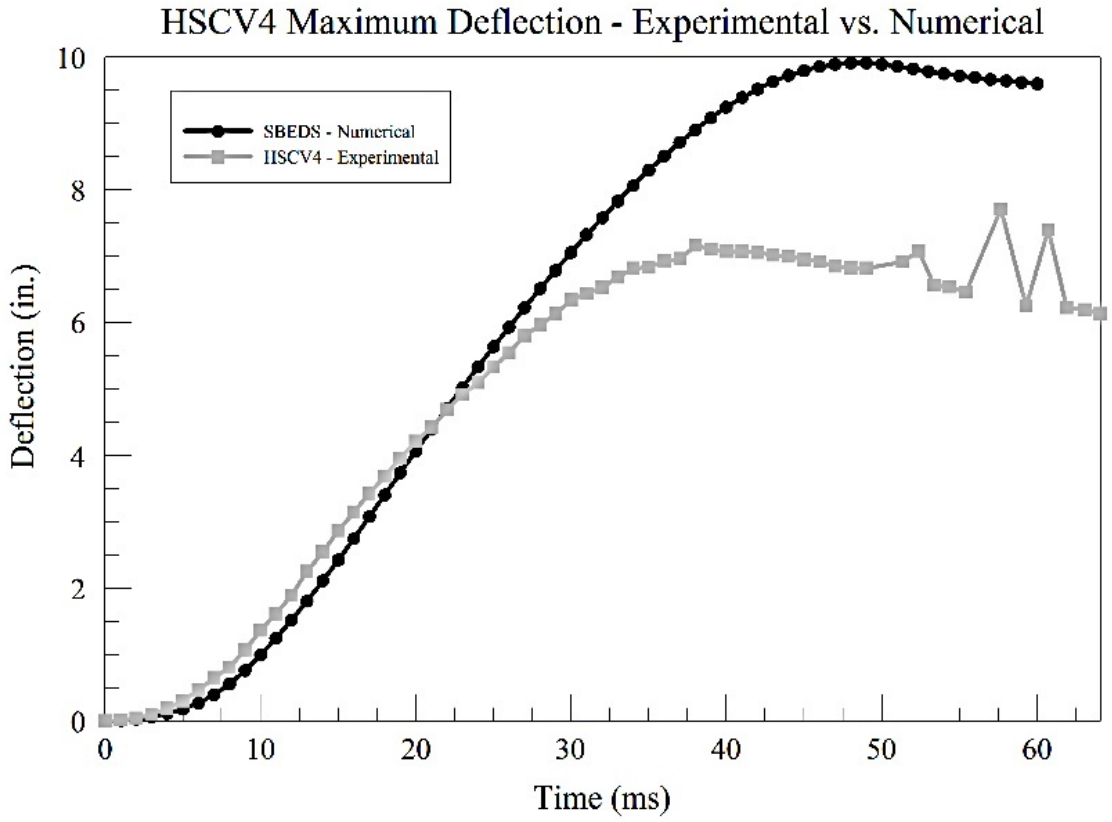

Figure 25- Maximum Experimental Deflection vs. SBEDS Actual Pressure-Time History Maximum Numerical Deflection for Slab HSCV4

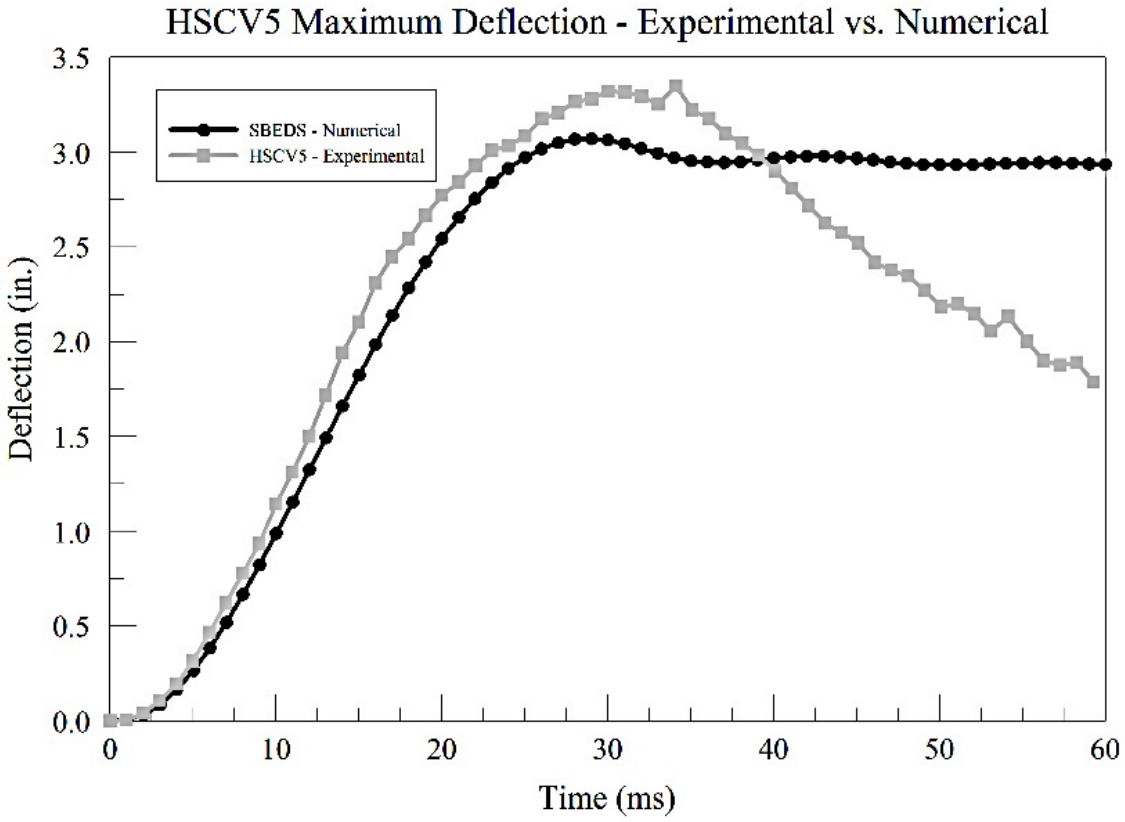

Figure 26- Maximum Experimental Deflection vs. SBEDS Actual Pressure-Time History Maximum Numerical Deflection for Slab HSCV5

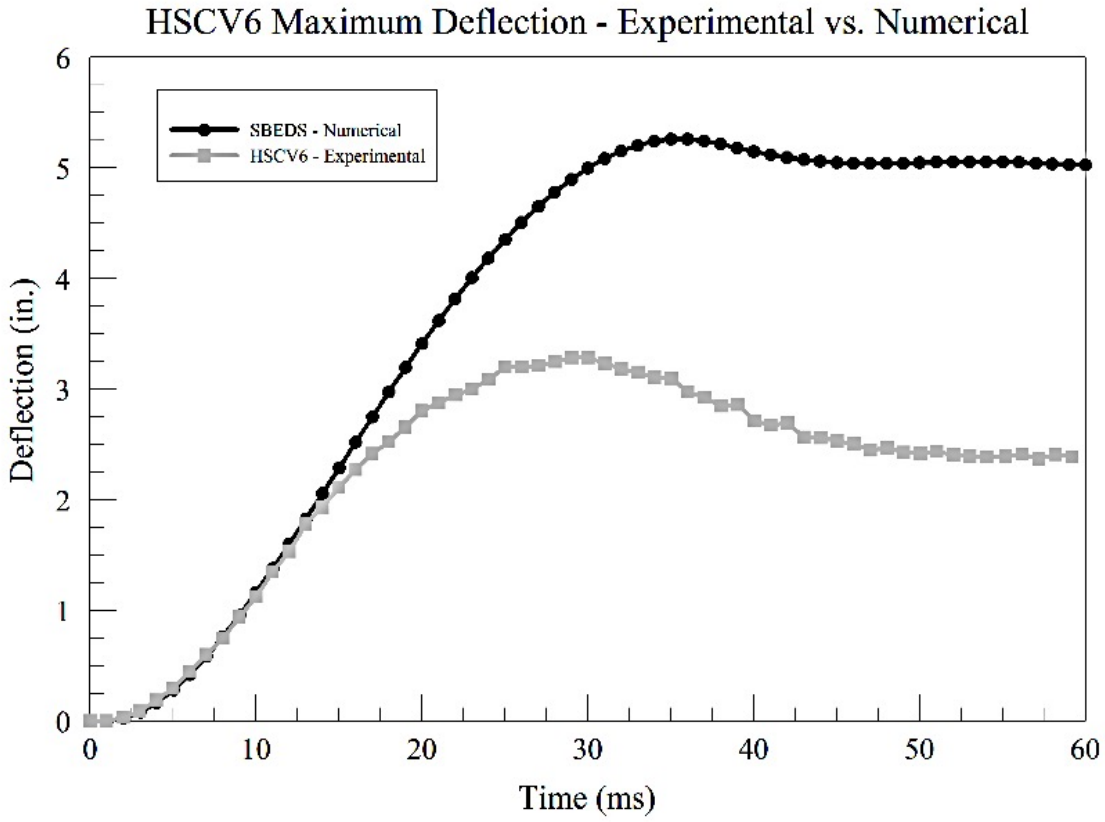

Figure 27- Maximum Experimental Deflection vs. SBEDS Actual Pressure-Time History Maximum Numerical Deflection for Slab HSCV6

In conclusion, SBEDS gave a better prediction of deflection values for the 8 in. (203.2 mm) slabs versus the 4 in. (101.6 mm) slabs established by observed experimental behavior. The maximum numerical deflection values obtained from the experimental pressure-time history SBEDS analysis and the PH1 and PH2 SBEDS analysis were smaller and less accurate, compared to those observed experimentally for the 4 in. (101.6 mm) slabs. Both of the SBEDS analyses produced maximum numerical deflection values that were more accurate and comparable to those observed experimentally for the 8 in. (203.2 mm) slabs. Therefore, it can be concluded, that the maximum numerical deflections obtained from SBEDS using the actual experimental pressure-time histories for each slab are more accurate in terms of what the slabs experienced experimentally for the 8 in. (203.2mm) slabs than for the 4 in. (101.6 mm) slabs. Therefore, it can be deduced for future designers using SBEDS to expect approximately 90% smaller deflections for slabs with 4 in. (101.6 mm) reinforcement spacing and 39% larger deflections for slabs with 8 in. (203.2 mm) reinforcement spacing to be reported from SBEDS compared to what will be observed experimentally. Based on the observations, it is also a possible conclusion that designers can expect more accurate deflections to be reported from SBEDS for slabs with larger reinforcement spacings.

CHAPTER 7

PARAMETRIC STUDY

In the parametric study conducted for this thesis, SDOF models were created for 4 in. (101.6 mm), 6 in. (152.4 mm), and 8 in. (203.2 mm) thick slabs with 2 in. (50.8 mm), 4 in. (101.6 mm), 6 in. (152.4 mm), 8 in. (203.2 mm), and 10 in. (254 mm) center-to-center reinforcement spacings.. A single average pressure time history was input into the SDOF model and was generated using the actual experimental pressure time histories for both the 4 in. (101.6 mm) and 8 in. (203.2 mm) slabs. Finally, the maximum numerical deflection obtained from SDOF analysis was studied to determine the effect of these varying parameters on the slab behavior when subjected to blast loading and was then compared to the maximum actual experimental deflection.

Slab Thickness and Reinforcement Ratio Variable Study

The parametric study was performed using SBEDS. Slab thickness and reinforcement spacing along with their corresponding effects on maximum deflection were analyzed. The maximum pressures and times of maximum pressure for HSCV1, HSCV2, HSCV3, HSCV4, HSCV5, and HSCV6 were averaged and entered into SBEDS. In order to provide a better overall synopsis of the scope and due to the limitations inherent in SBEDS, it was decided to input the overall average pressure time histories rather than subjected pressure time histories that would be more reflective of the various slab thicknesses and reinforcement ratios. Similarly, the pressures at 0 ms, 10 ms, 20 ms, 30 ms, 40 ms, 50 ms, and 60 ms for HSCV1, HSCV2, HSCV3, HSCV4, HSCV5, and HSCV6 were averaged and entered into SBEDS.

These pressure and time values can be observed in Table 11. The only variable parameter studied in this parametric study was maximum numerical deflection. The maximum numerical deflections obtained from SBEDS for the different slab thicknesses and reinforcement spacings can be seen in Tables 12-14.

Table 11 – Average Pressure Time History Data Input into SBEDS for Slab Thickness and Reinforcement Ratio Variable Study

Time, ms	Pressure, psi (kPa)
0	6.02 (41.5)
5.58	41.05 (283.0)
10	27.45 (189.3)
20	12.37 (85.3)
30	10.08 (69.5)
40	6.43 (44.3)
50	3.39 (23.4)
60	0 (0)

In general, from the SBEDS analysis, as the thickness of the slabs increased, the maximum numerical deflection reported from SBEDS decreased. The 4 in. (101.6 mm) thick slabs had the most variability, a variability of 118.2, in the maximum numerical deflections reported from SBEDS with 0.04 in. (1.02 mm) for 2 in. (50.8 mm) c/c reinforcement spacing and 25.59 in. (650 mm) for 10 in. (254 mm) c/c reinforcement spacing. SBEDS reported an

average maximum numerical deflection of 7.62 in. (193.5 mm) for the 4 in. (101.6 mm). The 6 in. (152.4 mm) thick slabs had the second most variability, a variability of 4.88, in the maximum numerical deflections reported from SBEDS with 0.03 in. (0.76 mm) for 2 in. (50.8 mm) c/c reinforcement spacing and 5.17 in. (131.3 mm) for 10 in. (254 mm) c/c reinforcement spacing. SBEDS reported an average maximum numerical deflection of 1.3 in. (33 mm) for the 6 in. (152.4 mm). The 8 in. (203.2 mm) thick slabs had the least variability, a variability of 0.23, in the maximum numerical deflections reported from SBEDS with 0.02 in. (0.51 mm) for 2 in. (50.8 mm) c/c reinforcement spacing and 1.10 in. (27.9 mm) for 10 in. (254 mm) c/c reinforcement spacing. SBEDS reported an average maximum numerical deflection of 0.25 in. (6.34 mm) for the 8 in. (203.2 mm). While the 8 in. (203.2 mm) thick slab had the least variability in maximum numerical deflection overall it also had the greatest increase in value, approximately fifteen times, between the maximum numerical deflection predicted by SBEDS for the 8 in. (203.2 mm) c/c reinforcement spacing and the 10 in. (254 mm) c/c reinforcement spacing. Similarly, the 6 in. (152.4 mm) thick slab which had the second least amount of variability, had the second greatest increase in value for maximum numerical deflection predicted by SBEDS between the 6 in (154.2 mm) and 8 in. (203.2 mm) c/c reinforcement spacing. This is unexpected due to the thickness of the concrete slabs and it is assumed that this is due to some internal programming error with reinforcement ratio when calculating the maximum numerical deflection for thicker slabs. This is another expectation that future designers could have when using SBEDS.

In general, from the SBEDS analysis, as the center-to-center spacing between the reinforcing bars increased, the maximum numerical deflection reported from SBEDS decreased. The 2 in. (50.8 mm) c/c reinforcement spacing yielded the least maximum

numerical deflection and the 10 in. (254 mm) c/c reinforcement spacing yielded the greatest maximum numerical deflection of all of the center-to-center reinforcement spacings. SBEDS predicted similar maximum numerical deflections for all 3 slab thicknesses for the 2 in. (50.8 mm) c/c reinforcement spacing slab with an average maximum numerical deflection of 0.03 in. (0.76 mm). SBEDS, again, predicted similar maximum numerical deflections for all 3 slab thicknesses for the 4 in. (101.6 mm) c/c reinforcement spacing slab with an average maximum numerical deflection of 0.153 in. (3.89 mm). SBEDS predicted fairly similar maximum numerical deflections for all 3 slab thicknesses for the 6 in. (154.2 mm) c/c reinforcement spacing slab with an average maximum numerical deflection of 0.68 in. (17.27 mm). SBEDS predicted maximum numerical deflections with a fair amount of variability, a variability of 31.3, for all 3 slab thicknesses for the 8 in. (203.2 mm) c/c reinforcement spacing slab with an average maximum numerical deflection of 3.81 in. (96.77 mm). SBEDS predicted maximum numerical deflections with the most amount of variability, a variability of 172, for all 3 slab thicknesses for the 10 in. (254 mm) c/c reinforcement spacing slab with an average maximum numerical deflection of 10.6 in. (269.24 mm). Of all of the center-to-center reinforcement spacing, the largest jump in maximum numerical deflection was observed from 8 in. (203.2 mm) to 10 in. (254 mm) c/c reinforcement spacing. Look at tables 12-14, it can be seen that between all 3 slab thicknesses, there is an average increase of almost 7 times the maximum numerical deflection for the 8 in. (203.2 mm) c/c reinforcement spacing slab for the 10 in. (254 mm) c/c reinforcement spacing slab.

Overall, the maximum numerical deflection produced by SBEDS increased with decreasing slab thickness and increasing center-to-center reinforcement spacing and reinforcement ratio. I.e. the 4 in. (101.6 mm) thick slab with 10 in. (254 mm) c/c reinforcement

spacing had the greatest maximum numerical deflection and the 8 in. (203.2 mm) thick slab with 2 in. (50.8 mm) c/c reinforcement spacing had the least amount of maximum numerical deflection predicted by SBEDS. All together, future designers using SBEDS can expect the maximum numerical deflection to decrease, on average, by 82% with every 2 in. (50.8 mm) of added slab thickness. They can also expect the maximum numerical deflection to decrease 3 times with every added 2 in. (50.8 mm) of center-to-center reinforcement spacing. Comparing the results from the parametric study to those observed experimentally similar conclusions are drawn as those obtained from the previous SBEDS studies. The maximum numerical deflections obtained from SBEDS were much lower and less accurate for the 4 in. (101.6 mm) c/c reinforcement spacing slabs than they were for the 8 in. (203.2 mm) c/c reinforcement spacing slabs.

Table 12 – Maximum Numerical Deflection from SBEDS for 4 in. Thick Slab and Variable Reinforcement Spacing

4 in. Thick Slab	
Spacing, s, in.	Maximum Deflection, x_{max},in. (mm)
2	0.04 (1.0)
4	0.34 (8.6)
6	1.9 (48.3)
8	10.24 (260.1)
10	25.59 (651.0)

Table 13 - Maximum Numerical Deflection from SBEDS for 6 in. Thick Slab and Variable Reinforcement Spacing

6 in. Thick Slab	
Spacing, s, in.	Maximum Deflection, x_{max},in. (mm)
2	0.03 (0.8)
4	0.09 (2.3)
6	0.11 (2.8)
8	1.12 (28.4)
10	5.17 (131.3)

Table 14 - Maximum Numerical Deflection from SBEDS for 8 in. Thick Slab and Variable Reinforcement Spacing

8 in. Thick Slab	
Spacing, s, in.	Maximum Deflection, x_{max}, in. (mm)
2	0.02 (0.5)
4	0.03 (0.8)
6	0.03 (0.8)
8	0.07 (1.8)
10	1.10 (27.9)

From the observations made from the parametric study, it can clearly be seen that thicker slabs with closer center-to-center reinforcement spacing experienced the least maximum numerical deflection. Unfortunately, none of the slabs with varying thicknesses and reinforcement ratios analyzed in SBEDS closely mimicked the maximum deflection of the actual slabs in the experiments. However, some useful conclusions were made from the parametric study and from the additional SDOF model maximum deflection study. From the experimental maximum deflections experienced by the 4 in. (101.6 mm) and 8 in. (203.2 mm) slabs and the numerical maximum deflections obtained from the analysis using the actual experimental pressure time histories experienced by the slabs, there are expectations that future designers should consider when using SBEDS as an analysis tool. First, when examining 4 in. (101.6 mm) thick high strength concrete slabs reinforced with Vanadium steel at 4 in. (101.6 mm) center-to-center spacing, designers could expect a much higher, up to nine times, increase in maximum experimental deflections, compared to those numerically obtained using SBEDS.

Second, when examining 4 in. (101.6 mm) thick high strength concrete slabs reinforced with Vanadium steel at 8 in. (203.2 mm) center-to-center spacing, designers could expect an approximate 25% decrease in maximum experimental deflections compared to those numerically obtained using SBEDS. In other words, SBEDS predicted an average maximum deflection that is 90% less than what the 4 in. (101.6 mm) slabs actually withstood and 28% more than what the 8 in. (203.2 mm) slabs actually withstood. Finally, it should be noted that there is particular variability in SBEDS when it comes to entering certain parameters such as reinforcement spacing and it is difficult to expect and closely match pressure-time histories with maximum deflections.

CHAPTER 8

COMPARISON OF HIGH STRENGTH CONCRETE SLABS WITH REGULAR STRENGTH CONCRETE SLABS

In this section, the six high strength concrete slabs reinforced with vanadium steel bars (HSCV), analyzed for this thesis, are compared with the six regular strength concrete slabs reinforced with regular steel bars (RSCR) which were analyzed previously by Thiagarajan and Johnson (15). HSCV1, HSCV2, and HSCV3 are compared with RSCR1, RSCR2, and RSCR3. These slabs had 4 inch (101.6 mm) longitudinal reinforcement spacing. HSCV4, HSCV5, and HSCV6 are compared with RSCR4, RSCR5, and RSCR6. These slabs all had 8 inch (203.2 mm) longitudinal reinforcement spacing. Table 15 shows the comparative details of the experimental data for the two types of slabs.

Table 15 – Recorded Experimental Data for Average Reflected Peak Pressure, Average Impulse, Peak Deflection, and Residual Deflection Values for all RSCR and HSCV Slabs

Slab No.	Average Peak Pressure, psi (kPa)		Average Impulse, psi-msec (kPa-msec)		Experimental Peak Deflection, in. (mm)		Experimental Residual Deflection, in. (mm)	
	RSCR	HSCV	RSCR	HSCV	RSCR	HSCV	RSCR	HSCV
1	53.1 (366.1)	49.7 (342.7)	976.2 (6730.7)	1013.3 (6986.5)	4.29 (109.0)	3.89 (98.8)	3.36 (85.3)	2.02 (51.3)
2	52.4 (361.3)	49.2 (339.2)	1000.4 (6897.5)	997.6 (6878.2)	4.45 (113.0)	4.50 (114.3)	3.32 (84.3)	3.50 (88.9)
3	44.2 (304.7)	39.9 (275.1)	785.3 (5414.5)	773.9 (5335.8)	3.17 (80.5)	2.47 (62.7)	1.96 (49.8)	1.37 (34.8)
4	33.4 (230.3)	41.1 (283.4)	494.4 (3408.8)	753.9 (5198.0)	3.36 (85.3)	7.16 (181.8)	3.19 (81.0)	5.59 (142.0)
5	34.8 (239.9)	31.0 (213.7)	549.5 (3788.7)	511.6 (3527.4)	3.6 (91.4)	3.4 (86.4)	1.58 (40.1)	1.53 (38.9)
6	33.7 (232.4)	35.4 (244.1)	509.0 (3509.4)	576.1 (3972.1)	3.17 (80.5)	3.38 (85.8)	1.94 (49.3)	1.9 (48.3)

Experimental Peak Deflection

HSCV1, HSCV2, RSCR1, and RSCR2 were all subjected to the highest peak average pressure and average impulse values and their experimental peak deflections reflect this. HSCV1 had an experimental peak deflection of 3.89 inches (99 mm) while HSCV2 had a larger experimental peak deflection of 4.50 inches (114 mm). RSCR1 and RSCR2 had experimental peak deflections of 4.29 inches (109 mm) and 4.45 inches (113 mm), respectively. This indicates that the RSCR slabs exhibited, approximately, 4% higher peak experimental

deflection values than the HSCV slabs. The effect of increased concrete strength was not significant.

HSCV3, HSCV4, RSCR3, and RSCR4 were subjected to lower average peak pressure and average impulse values than the previous slabs and their experimental peak deflection values, for the most part, reflect this well. HSCV3 had an experimental peak deflection value of 2.47 inches (63 mm) while HSCV4 had a significantly higher experimental peak deflection value of 7.16 inches (182 mm). This is expected because of the larger longitudinal reinforcement spacing and the higher peak pressure subjected to HSCV4. RSCR3 and RSCR4 had experimental peak deflection values of 3.17 inches (81 mm) and 3.36 inches (85 mm), respectively. This indicates that the HSCV slabs exhibited, approximately, 39% higher experimental peak deflection values than the RSCR slabs. This large difference percentage is due to the erroneous experimental peak deflection experienced by HSCV4. By removing the one large deflection value it can be seen that the HSCV slabs experience 24% less deflection than the RSCR slabs. It should also be mentioned that, when comparing the observed maximum peak pressures and deflections, HSCV3 experienced a 22% less peak deflection value when subjected to a 10% lesser peak pressure than RSCR3. Similarly, HSCV4 experienced a 113% larger peak deflection value when subjected to a 23% greater peak pressure than RSCR4. This is an acceptable result.

HSCV5, HSCV6, RSCR5, and RSCR6 were all subjected to the lowest average peak pressure and average impulse values and their experimental peak deflection values reflect this well. HSCV5 had an experimental peak deflection of 3.4 inches (86 mm) and HSCV6 experienced a similar experimental peak deflection value of 3.38 inches (86 mm). RSCR5 and RSCR6 had experimental peak deflection values of 3.6 inches (91 mm) and 3.17 inches (81

mm), respectively. This indicates that the HSCV slabs and the RSCR slabs had similar experimental peak deflection values, with the HSCV slabs having only, approximately, 0.15% higher values than the RSCR slabs, once again indicating that the higher concrete strengths did not significantly affect the results.

Crack and Damage Patterns

The crack patterns for the six HSCV slabs exhibited similar characteristics to the crack patterns of the six RSCR slabs, as described in Thiagarjan and Johnson's work (15). HSCV1, HSCV2, RSCR1, and RSCR2 were subjected to the highest pressure and impulse values and extensive tensile cracking with clear crushing of concrete can be observed on the blast face. HSCV4, HSCV5, RSCR4, and RSCR5 were subjected to lower pressure and impulse values and did not crack as much in tension and they did not show a significant amount of compression crushing. HSCV3, HSCV6, RSCR3, and RSCR6 were subjected to lower pressure and impulse values in which lower levels of both tension and compression crushing can be observed. In general, there was no visible cracking observed at the strain gauge levels in all the slabs, suggesting that the confidence in the strain values and that the gauges were not damaged and held up through the process. The crack and damage patterns for HSCV2, HSCV3, HSCV4, and HSCV5 are shown in Figures 28, 29, 30, and 31, respectively.

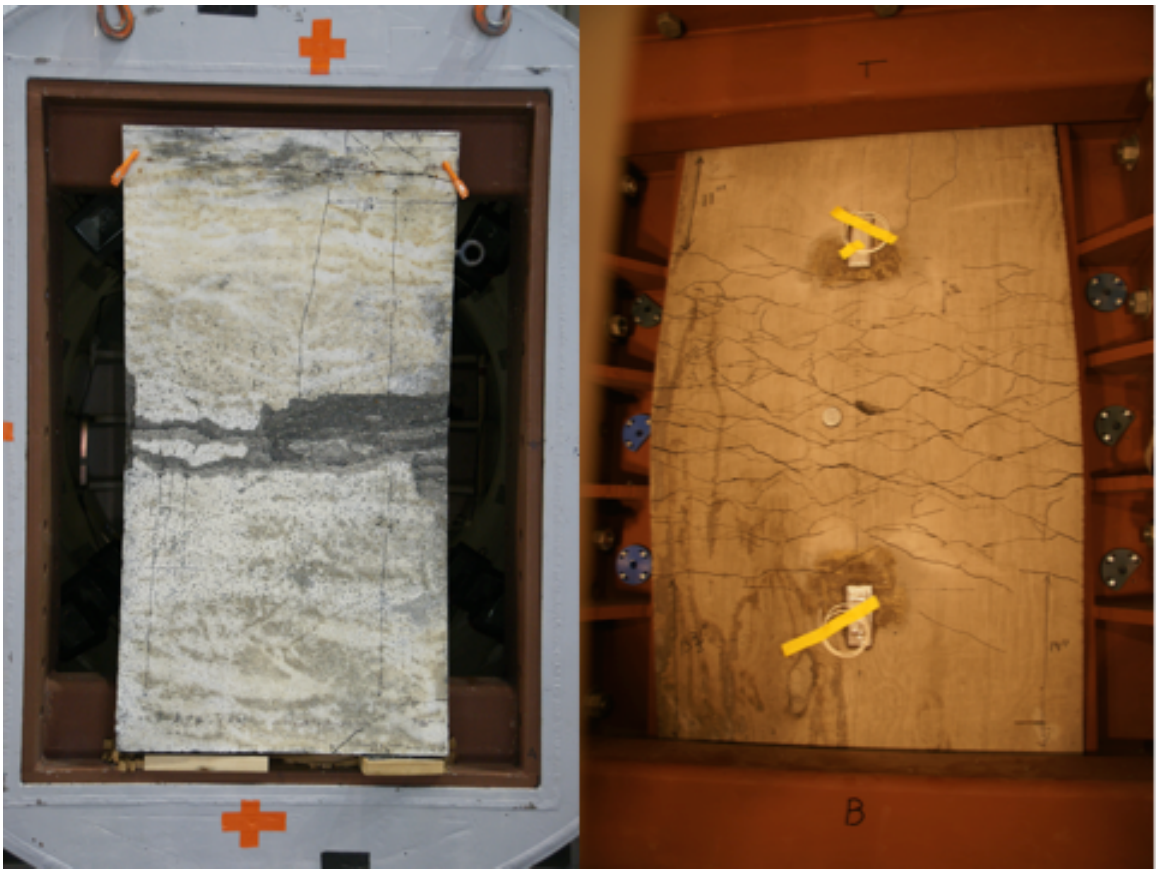

Figure 28- Damage to HSCV2 (4 in. [101.6 mm] Spacing; P = 49.2 psi [339.2 kPa]; I = 997.6 psi-msec [6878.2 kPa-msec]).

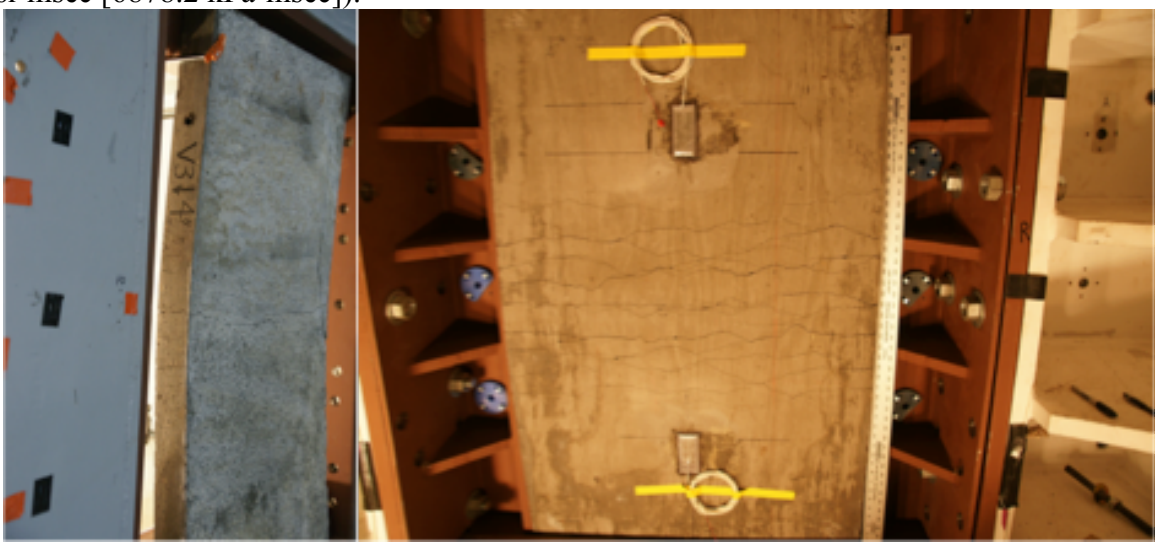

Figure 29- Damage to HSCV3 (4 in. [101.6 mm] Spacing; P = 39.9 psi [275.1 kPa]; I = 773.9 psi-msec [5335.8 kPa-msec]). Damage to Blast Face (Left) and Back Face (Right).

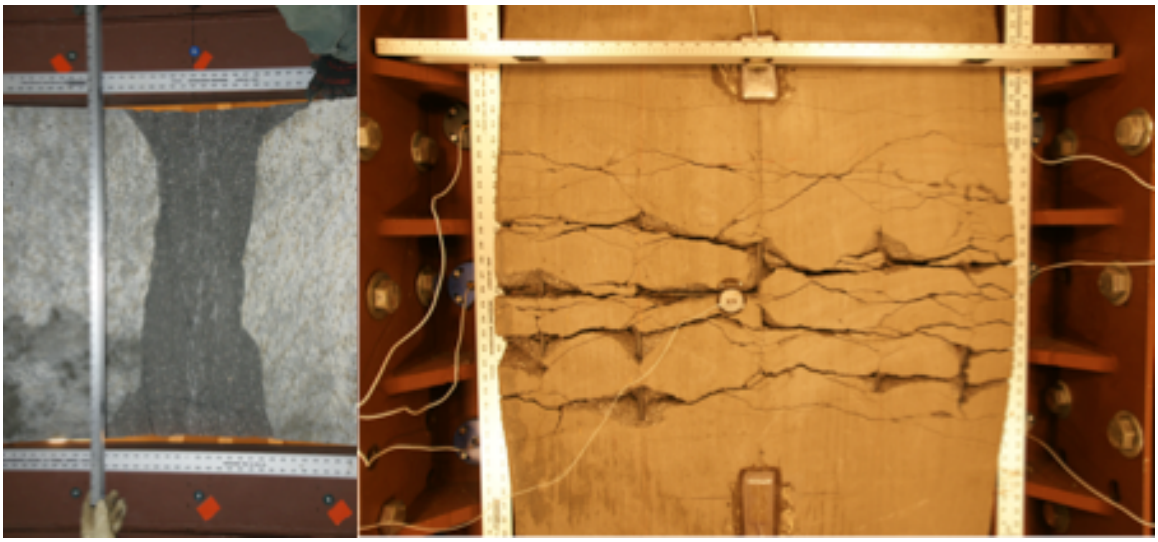

Figure 30- Damage to HSCV4 (8 in. [203.2 mm] Spacing; P = 41.1 psi [283.4 kPa]; I = 753.9 psi-msec [5198.0 kPa-msec]). Damage to Blast Face (Left) and Back Face (Right).

Figure 31- Damage to HSCV5 (8 in. [203.2 mm] Spacing; P = 31.0 psi [213.7 kPa]; I = 511.6 psi-msec [3527.4 kPa-msec]). Damage to Blast Face (Left) and Back Face (Right).

CHAPTER 9

CONCLUSIONS

Air blast tests that have been conducted on one-way, high strength RC panels with two different vanadium steel reinforcement ratios provided ample experimental results. The panels were able to withstand the imposed design impulses and pressures without exhibiting signs of complete and catastrophic failure. Strain and deflection histories were generated from the tests performed on the panels and, based on this experimental data, along with the numerical studies conducted for this research, the following conclusions are made:

1. The peak deflections observed for the 4 in. (101.6 mm) slabs were, approximately, 10 times the peak deflections predicted by SBEDS. However, the peak deflections predicted by SBEDS for the 8 in. (203.2 mm) slabs were, approximately, 1.307 times the peak deflections observed experimentally. These observations suggest that the 4 in. (101.6 mm) spacing slabs performed better than the 8 in. (203.2 mm) spacing slabs in terms of having a lower deflection response when subjected to higher pressures.

2. The design curves corresponding to the various levels of protection (LOP) for the 8 in. (203.2 mm) slabs are conservative compared to the experimental damage levels (the design PI values per SBEDS are much lower than what the slabs can actually withstand) while only the MHLOP design curve showed this same level of conservatism for the 4 in. (101.6 mm) slabs. It can be concluded that there is sufficient conservatism built into the design curves developed using

SBEDS for the 8 in. (203.2 mm) slabs and modest conservatism is built into the design curves using SBEDS for the 4 in. (101.6 mm) slabs.

3. The observations indicate the critical importance of spacing restrictions in the design of slabs subjected to blast loading. The 4 in. (101.6 mm) slabs developed higher post yield strengths along with higher ductility values than the 8 in. (203.2 mm) slabs. Further softening of the 4 in. (101.6 mm) slabs was observed from the plots shown in Figures 18 and 19 than the 8 in. (203.2 mm slabs). Observed experimental dynamic resistance for the slabs was higher than that exhibited by SBEDS. Peak deflection values predicted using SBEDS proved to be higher for the 8 in. (203.2 mm) slabs. Futhermore, the peak deflections obtained from the SBEDS parametric study confirm that smaller reinforcement spacing, along with larger slab thicknesses, results in more favorable slab behavior when subjected to shock loading.

4. Based on the observations it could be concluded that the usage of high strength concrete and reinforcement offered some advantages over regular concrete and steel. However, the spacing of reinforcement played a more significant role.

Based on the results from the research presented in this thesis, for the HSCV slabs, and the research from the previous paper, for the RSCR slabs, the limitations of these experimental studies are as follows. Only one-way slab with two reinforcement ratios and one slab thickness were investigated. Future research should address all these aspects as well as devise frames that could study the behavior of columns and two-way slabs, which are critical components in protective structure designs. Overall, the design of experiments and the tests conducted were

satisfactory. The experimental data and the comparison of the data with commonly used design methods such as the SDOF method predictions are valuable tools for both researchers and designers to compare their numerical models or to assess their designs of similar systems.

REFERENCES

1. Smith SJ, McCann DM, Kamara ME, "Blast Resistant Design Guide for Reinforced Concrete Structures." Skokie,Illinois: Portland Cement Association; 2009.

2. Karthaus W, Leussink J, "Dynamic loading: More than just a dynamic load factor," Book Dynamic loading: More than just a dynamic load factor, Editor, ed.^eds., Prins Maurits Laboratorium Tno Rijswijk (Netherlands), City, 1983, pp. 10-4.

3. Baylot JT, Bevins TL, "Effect of responding and failing structural components on the airblast pressures and loads on and inside of the structure," Computers & Structures, V. 85, No. 11-14. 2007, pp. 891-910.

4. Malvar LJ, Ross CA, "Review of strain rate effects for concrete in tension," ACI Materials Journal, V. 95, No. 6. 1998.

5. Li Q, Meng H, "Pressure-Impulse diagram for blast loads based on dimensional analysis and single-degree-of-freedom model," Journal of Engineering Mechanics, V. 128. 2002, pp. 87.

6. Zhao C, Chen J, "Damage mechanism and mode of square reinforced concrete slab subjected to blast loading," Theoretical and Applied Fracture Mechanics, V. 63. 2013, pp. 54-62.

7. Yi N-H, Kim J-HJ, Han T-S, Cho Y-G, Lee JH, "Blast-resistant characteristics of ultra-high strength concrete and reactive powder concrete," Construction and Building Materials, V. 28, No. 1. 2012, pp. 694-707.

8. Yun S-H, Park T, "Multi-physics blast analysis of reinforced high strength concrete," KSCE J Civ Eng, V. 17, No. 4. 2013, pp. 777-88.

9. Wu C, Oehlers DJ, Rebentrost M, Leach J, Whittaker AS, "Blast testing of ultra-high performance fiber and FRP-retrofitted concrete slabs," Engineering structures, V. 31, No. 9. 2009, pp. 2060-9.

10. Du H, Li Z, "Numerical analysis of dynamic behavior of RC slabs under blast loading," Transactions of Tianjin University, V. 15, No. 1. 2009, pp. 61-4.

11. Li Q, Meng H, "Pulse loading shape effects on pressure-impulse diagram of an elastic-plastic, single-degree-of-freedom structural model," International Journal of Mechanical Sciences, V. 44, No. 9. 2002, pp. 1985-98.

12. Krauthammer T, Frye M, Schoedel T, Seltzer M, "Advanced SDOF approach for structural concrete systems under blast and impact loads," Book Advanced SDOF approach for structural concrete systems under blast and impact loads, Editor, ed.^eds., City, 2003, pp.

13. CEB, "Concrete structures under impact and impulsive loadings," Book Concrete structures under impact and impulsive loadings, 187, Editor, ed.^eds., Comite' Euro-International du Beton Lausanne, Switzerland (CEB Bulletin 187), City, 1988, pp.

14. ASCE, "Design of structures to resist nuclear weapons effects," Book Design of structures to resist nuclear weapons effects, Editor, ed.^eds., American Society of Civil Engineers (ASCE), City, 1985.

15. Thiagarajan G, Johnson CF, "Experimental behavior of reinforced concrete slabs subjected to shock loading " American Concrete Institute - Structural Journal, V. 111, No. 6, 11/1/2014. 2014, pp. 1407-18.

16. Grote D, Park S, Zhou M, "Dynamic Behavior of Concrete at High Strain Rates and Pressures: I. Experimental Characterization," International Journal of Impact Engineering, V. 25, No. 9. 2001, pp. 869-86.

17. Ross CA, Tedesco JW, Kuennen ST, "Effects of strain rate on concrete strength " ACI Material Journal, V. 92, No. 1. 1995, pp. 9.

18. Mays G, Smith PD, "Blast effects on buildings: Design of buildings to optimize resistance to blast loading." Thomas Telford; 1995.

19. Morison CM, "Dynamic response of walls and slabs by single-degree-of-freedom analysis--a critical review and revision," International Journal of Impact Engineering, V. 32, No. 8. 2006, pp. 1214-47.

20. Nebuda D, "Single degree of freedom blast effects design spreadsheets," Book Single degree of freedom blast effects design spreadsheets, Editor, ed.^eds., City, 2005, pp. 2-4.

21. Ghani Razaqpur A, Tolba A, Contestabile E, "Blast loading response of reinforced concrete panels reinforced with externally bonded GFRP laminates," Composites Part B: Engineering, V. 38, No. 5-6. 2007, pp. 535-46.

22. Krauthammer T, "Blast mitigation technologies: Developments and numerical considerations for behavior assessment and design," Book Blast mitigation technologies: Developments and numerical considerations for behavior assessment and design, Editor, ed.^eds., Computational Mechanics Inc., City, 1998, pp. 1-10.

23. Shi Y, Hao H, Li Z, "Numerical derivation of Pressure-Impulse diagrams for prediction of RC column damage to blast loads," International Journal of Impact Engineering, V. 35, No. 11. 2008, pp. 1213-27.

24. USDOD, "United Facilities Criterion UFC 4-010-01," Book United Facilities Criterion UFC 4-010-01, Editor, ed.^eds., City, 2012, pp.

25. ASCE/SEI, "Blast protection of buildings," Book Blast protection of buildings, Editor, ed.^eds., American Society of Civil Engineers, City, 2011, pp.

26. Fallah AS, Louca L, "Pressure-Impulse diagrams for elastic-plastic-hardening and softening single-degree-of-freedom models subjected to blast loading," International Journal of Impact Engineering, V. 34, No. 4. 2007, pp. 823-42.

VITA

Kristen Ashley Reynolds was born on January 18th, 1991 in Kansas City, Missouri. She attended Shawnee Mission East High School in Prairie Village, Kansas. She then went on to study at the University of Missouri-Columbia where she graduated with a Bachelor of Science degree in Civil and Environmental Engineering in December 2013. After graduation, Kristen moved back to Kansas City and began her graduate education at the University of Missouri-Kansas City to obtain a Masters of Science degree in Structural Engineering, a subject which she has always been passionate about. While in school, Kristen has worked as a research and teaching assistant for Dr. Ganesh Thiagarajan where she has gotten the amazing opportunity to work, not only on blast design of concrete structures, but also closely with undergraduate students on unique reinforced concrete and structural steel material projects. She has just finished a summer internship at HNTB in Kansas City with the bridge group as the structural engineer intern. After graduation, Kristen has accepted a position with Olsson Associates as the Assistant Railroad Bridge Structural Engineer where she intends to continue her passion and further pursue her career in structural engineering.